DEMOCRATIC AND POPULAR REPUBLIC OF ALGERIA

Ministry of Higher Education and Scientific Research

University of Tlemcen

جامعة أبو بكر بلقايد

UNIVERSITÉ DE TLEMCEN

Pan African University
Institute of Water
and Energy Sciences

PAN AFRICAN UNIVERSITY

Institute for Water and Energy Sciences (Incl. Climate Change)

RUNOFF RESPONSE TO CLIMATE VARIABILITY: AN ANALYSIS OF THIKA RIVER BASIN IN KENYA

Student name: Michael Maina Macharia

Date: 28/08/2016

Master in ***Water Engineering track***

Members of Jury:

President

Supervisor: **Dr. (Eng.) James M. Raude**

Co-Supervisor: **Dr. Sidi Mohammed Chabane Sari**

Examiner 1

Academic Year: 2015-2016

This thesis is submitted in partial fulfillment for the requirements of MSc in Water Engineering at Pan African University Institute of Water and Energy Sciences (including Climate Change) (PAUWES) at the University of Tlemcen in Algeria.

September 2016.

DECLARATION

I, **Michael Maina Macharia** do hereby declare that this thesis is my original work and to the best of my knowledge, it has not been submitted for any award in any University or Institution.

Signed_____ Date _____

Michael Maina Macharia

CERTIFICATION

This thesis has been submitted with my approval as the supervisor

Signed_____Date_____

Dr. (Eng.) James M. Raude

Jomo Kenyatta University of Agriculture & Technology

Soil, Water and Environmental Engineering Department

ABSTRACT

Changes in climatic conditions have greatly affected surface runoff and stream flows both at local and global scale. This has led to adverse effects on surface run off and climatic system as a whole. Research on these hydrological changes at basin scale is of great importance to the water managers for the future planning and management of water resources. The Thika River catchment is of great importance to Kenya and plays host to Ndakaini Dam which provides about 84% of Nairobi's water supply to a population of over 3 million residents, whose contribution to Kenya's Gross Product is 60%. Observed climatic variability and trends for Thika catchment were assessed for significance with Mann Kendall's trend test and discussed in light of future climate variability scenarios. The results indicate that the catchment has become relatively warmer over the last four decades. The annual precipitation and means of daily mean temperatures over the past 30 years has increased by about 7.8 mm (although not statistically significant), and 2.14°C respectively. The trend for the annual mean of daily temperatures was statistically significant. Hydrological simulation model was used to simulate runoff and quantify the effects of climate variability on runoff within the area of study. The model was calibrated and validated giving a coefficient of determination (R^2) of 0.923, an RMSE of 0.56 and a BIAS of 1.697. The future climate of the catchment is projected to be warmer and, with less confidence, wetter. However, stream flow could increase by between 1.2% on the lower case to 4.5% on the higher case under these projections. There is therefore need to prepare for the increased runoff as it would affect the agricultural sector, industry, urban communities, as well as the environment.

Table of Contents

LIST OF FIGURES

LIST OF TEMPLATES

LIST OF TABLES

LIST OF ABBREVIATIONS AND ACRONYMS

A.M.S.L.	Above Mean Sea Level

ASAL	Arid and Semi-Arid Lands
ASCE	American Society of Civil Engineers
HEC	Hydrological Engineering Center
HEP	Hydro Electrical Power
HYSIM	Hydrological Simulation Model
IPCC	Intergovernmental Panel on Climate Change
KMD	Kenya Meteorological Department
MWI	Ministry of Water and irrigation
NCC	Nairobi City Council
NSE	Nash-Sutcliffe Efficiency
PET	Potential Evapotranspiration
R^2	Coefficient of Determination
RMSE	Root Mean Square Error
SAR	Second Assessment Report
SCS	Soil Conservation Service
SSARR	Stream flow Synthesis and Reservoir Regulation
SWBM	Storm Water Management Model
UK	United Kingdom
US	United States

CHAPTER ONE

INTRODUCTION

1.1. Background information

Changes in climatic conditions have greatly affected surface run off and stream flows both at local and global scale. This variability also impacts on the the functioning of water facilities in existence including flood control facilities, hydropower, irrigation and drainage facilities as well as water regulation practices (Michael & Cayan, 1995). The variations are a natural component of the climate which is caused by changes in the system(s) which influence the climate such as the General Circulation system. According to UNEP (2013) it has been observed periodically that Nile basin's weak system has given rise to extreme climate events due to variations in the various climate variability drivers. Climate variability drivers are elements that bring about a climatic variability, they include: precipitation distribution, temperature, soil moisture and evaporation.

Research on hydrological changes at basin scale is of great importance to the water managers for future policies formulation, planning and management of the resource. According to Box and Jenkins (1970), the traditional way of forecasting forthcoming climate conditions based on the assumption of past hydrological occurrences is no longer applicable. Adverse effects of meteorological conditions on drinking water systems aggravate the implications of other stresses, such as human population growth, changing economic activity, land-use change and urbanization (KMD, 2010). While quantitative projections of changes in rain, stream flows and water levels at the river-basin scale are uncertain, it is very likely that hydrological characteristics will change in the coming years (IPCC, 2014). Adaptation procedures and risk management policies that

incorporate projected hydrological changes with related uncertainties are being developed in several countries and regions (IPCC, 2014). The consequences of climate variability may alter the reliability of current water management systems and water-related facilities. These changes call for runoff modeling which takes into account the changing conditions. The runoff should be simulated under the different climate variability scenarios. Hydrological Simulation Model (HYSIM) was used in this study by incorporating the various scenarios as suggested by the IPCC to study the impacts of the climate variability in the basin.

According to Turral (2011), despite the great importance of climate variability and its impacts across many sectors of the economy, society, and the environment, there is little understanding of its extent in Kenya. This study was aimed at spearheading initiatives towards such understanding. The Thika River catchment is of great importance to Nairobi County in Kenya since the catchment provides 84% of water supply to a population of over three million residents whose contribution to Kenya's Gross Domestic Product from Nairobi alone is over 60% (Mogaka, 2006). It is a tributary to the Tana River which provides the bulk of the country's hydroelectricity power needs, irrigation needs as well as providing drinking water to millions of other individuals. Ndakaini Dam which provides about 84% of Nairobi's water supply is also located in this catchment (Athi, 2006). According to NEMA (2006), Kenya was mostly characterized by dry conditions in 1950s and early 1970s whereas wet conditions occurred in early 1960s and late 1980s. Recent extreme events include: droughts of 1984, 1990, 1994, and 1999 and El Nino floods in 1997/1998 (NEMA, 2006).

Temperatures in Kenya do not show large variation in its mean throughout the year but shows variation geographically, seasonally and diurnally due to altitude. The mean annual rainfall

depicts a wide spatial variation, which ranges from 200mm in the driest areas in northwestern and eastern parts of Kenya to the wetter areas with rainfall of 1200-2000 mm in areas which boarders Lake Victoria and central highlands east of the rift valley (Ndirangu, Kabubi, & Dulo, 2009). The Kenyan climate has evidenced natural disasters, with floods and droughts occurring periodically as result of rainfall anomalies. There has been in the past 50 years at least thirteen serious droughts and six major flooding which have affected Winam gulf of the Lake Victoria and the lower Tana area (NEMA, 2006).

1.2. Statement of the problem

Determining climate variability effects on surface runoff both on a local and regional scale helps in effective planning of the future water resources. According to IPCC (2000) temperature is expected to increase by between 0.2^{o}C and 0.5^{o}C consequently triggering a rainfall increase of about 5 to 20% during the wet months and 5 to 10% during the dry months. Determining these changes in runoff in both climate variability and climate change is not enough without taking into account the climate variability scenarios. Unfortunately, there is a major challenge in taking account of climate change scenarios making it hard to significantly determine climate variability effects. This leads to use of assumptions on the climate change effects resulting to wrong data when predicting surface runoff (Arnell, 2003). The outcome of wrong assumptions compromises future planning of water resources.

According to Hulme et al. (2001), there are two main reasons why there is little confidence about the magnitude, and even direction, of regional rainfall changes in Africa. The first reason relates to ambiguous representation of climate variability in the tropics. This is in most GCMs via mechanisms such as ENSO, for example, which is a key determinant of African rainfall

variability. The second reason is the omission in all current global climate models of any representation of dynamic land cover–atmosphere interactions. These interactions have been suggested to be vital in determining climate variability in Africa during Holocene and may also have played a role to the more recently observed desiccation of the Sahel (Hulme et al. 2001). Work is now underway however, to incorporate such links in regional climate models (Moore et al. 2009).

Unless credible models are used, the problem cannot be effectively solved. Hydrological models have been used in exploring the implication of making certain assumptions about the real world system and predicting the behavior of the real system under a set of naturally occurring circumstances. This research used the HYSIM model to overcome the challenge of taking into account climate variability scenarios while accessing runoff within the Thika river catchment.

1.3. Study justification

Over recent years there has been increasing evidence that the earth's climate will become warmer in 21st century, which raises the essential question: What impacts will global warming have on the environment and human activities (IPCC et al., 2000). Global warming will lead to hydrologic changes that will affect freshwater resources including surface runoff. These are among the most significant potential impacts of climate change and variability. As the climate warms, changes in the nature of global precipitation, evaporation, snowpack, stream flow and other factors that will affect freshwater supply and quality will be evidenced. According to Athi (2006), Thika River not only provides water to power the energy needs of the country but also 84% of its water needs to drive Nairobi, the country's capital city. Nairobi is periodically faced with serious water shortages as water levels in Ndakaini Dam hit unprecedented low levels

during dry spells. The energy situation is made worse by frequent low water levels at Masinga dam along the Tana River which leads to shut downs. All this has come about due to the serious changes and variability in climate. Kenya was faced with the worst dry spell in early 2015 followed by a season of extreme rainfall events. Climate variability and change will present challenges to water utilities, and developing mitigation now could prevent freshwater crises in upcoming years (KMD, 2010). Determination of the effect of climate variability on surface runoff in Thika catchment helps the country to be in a position to determine future floods or drought and predict possible future trends to enable formulation of mitigation and preparedness measures. Exploring vulnerability means extreme events providing most important message needed for impact prediction, analysis and development of mitigation measures.

1.4. Objectives

1.4.1 General objective

The main objective of this study was to evaluate the response of surface runoff due to climate variability in Thika river basin in Kenya using hydrological simulation model.

1.4.2 Specific objectives:

The specific objectives are to:

i. Calibrate and validate HYSIM model's ability to simulate surface runoff through use of rainfall, stream flow, and PET data for the period between 1960 and 1995.

ii. Simulate changes in runoff from different climate variability scenarios developed by IPCC with weather data, stream flow data and topological maps.

iii. Analysis of the trends in temperature and rainfall generated in the catchment based on the climatic data for the period starting 1976 to 2006.

1.5. Research Questions

Research questions were;

a) How does surface runoff in the catchment respond due to climate variability?

b) How can HYSIM be used in runoff simulation in a watershed?

c) Are there any trends in temperature and rainfall generated in the catchment?

1.6. Scope and limitations of the study

The area that was under this study is Thika river catchment. The main river in this catchment is Thika River which is part of the larger Tana catchment. HYSIM model was used to simulate surface runoff from the available weather data and hence thereafter the results evaluated**.** The model used a 15 years' dataset in batches of 5 years each three stream flow gauging stations within the catchment.

CHAPTER TWO

LITERATURE REVIEW

2.1 General introduction

In 1997, the UN Comprehensive Assessment of the Freshwater Resources of the World (WMO, 1997) gave estimations that a third of the world's population was living in countries suffering from water stress. This meant that the populations in these countries were drawing more than 20% of the water resources available. The report also came up with estimations that by 2025, two thirds of the world population would be living in water stressed countries. With the increasing levels of greenhouse gases (GHG), the volume and timing of the runoff and ground recharge will be affected. This will have a great impact on the number of people who are affected by water scarcity. The estimates on the impact of climate change are based on the assumed emissions scenarios, climate models and the assumed changes in population (Luijten, 1999). This means that climatic conditions will vary along with time (IPCC et al., 2000).

In a study by Lukeman (2003), it is reported that the main drivers of Climate variability include precipitation distribution, soil moisture, evaporation and temperature. Other drivers of weather and climate variability include solar energy from the sun, earth's pressure systems, moisture sources, sea/ocean land interface, the surface albedo, the topography and relief (Ndirangu, Kabubi, & Dulo, 2009). Climate variability implies variations in the mean state and other climate statistics such as standard deviations, the occurrence of extremes amongst others on all temporal and spatial scales beyond those of individual weather events. Universal climatic variability may be resulting from internal natural processes or perhaps even external processes. Global climate warming is the increase of earth's near-surface air and ocean temperatures which is usually as a result of the accumulation of more and more greenhouse gases resulting from anthropogenic

pursuits like burning of fossil fuels (NEMA, 2014). It is essential to note from the above definition that global climatic change, climatic variability and global climate warming are not quite the same though closely related.

2.2 Climate Variability

Based on the Millennium Ecosystem Assessment (2005), natural hazards and disasters are products of both natural variability and human–environment interactions. It is important to note that extremes in variability are defined as hazards when they represent threats to people and what they value and defined as disasters when an event overwhelms local capacity to cope. There is little information on changes in African climate variability (Sivakumar et al. 2005; Christensen et al. 2007). The increase in African rainfall is associated partly with an increase in atmospheric water vapor. The increase in number of wet seasons is estimated to be at 20% (Christensen et al. 2007).

2.2.1 Reasons for climate variability and its factors

Climate variability changes as a consequence of a several variables. These variables are; interface between ocean and the atmosphere, changes in the world's orbit and changes in energy from the sun. There is proof that the late global warming is not only attributable to natural variables but rather human causes which appear to be the significant cause (IPCC, 2013). The progressions seen over late years and those anticipated for the following century are taken to be mostly the consequence of human conduct through interaction with the environment. Human activity is the primary driver of the changes found in atmosphere in the recent decades.

The earth has warmed by 0.75 degrees Celsius in the most recent 100 years globally and ocean levels have gone up (Stocker *et al.,* 2014). Extreme weather, such as floods and dry spells, are likely to happen regularly resulting in immediate direct and indirect impacts. These can lead to flare-up of ailments such as Malaria (Hay *et al.,* 2002). The increase in carbon dioxide concentration worldwide are significant because of fossil fuel usage and land use change, while those of methane and nitrous oxide are principally because of agribusiness that generally comes about from the production process utilizing animals (IPCC, 2007).

Unlike weather which varies day to day, climate varies seasonally. Some summers are colder than others while some years have high overall precipitation. Climate variability is not as noticeable as weather variability since it happens over seasons and years. Common drivers for climate variability are El Nino and La Nina events, volcanic eruptions and sunspots. El Nino and La Nina events are shifts of warm tropical Pacific Ocean currents (Hay *et al.*, 2002).

2.3 Classification of Climate Variability

Climate variability can be classified into two major sub-groups depending on their causes;

a) Natural variability: This is the disparity in the various components of climate resulting from the effects of natural processes. For example, the natural greenhouse effect where the natural greenhouse gases and clouds cause changes in temperatures and also in the solar radiation (Fu *et al.,* 2009).

b) Anthropogenic variability: This is the variation resulting from impact of Human activities for instance the burning of fossil fuel resulting into the alteration of the composition of the atmosphere. A good example is through land use changes such as urbanization, deforestation, construction of land water reservoirs (Lukeman, 2003).

There are several forms of climate variation as can be seen in Figure (2.1) after Fu *et al.* (2009).

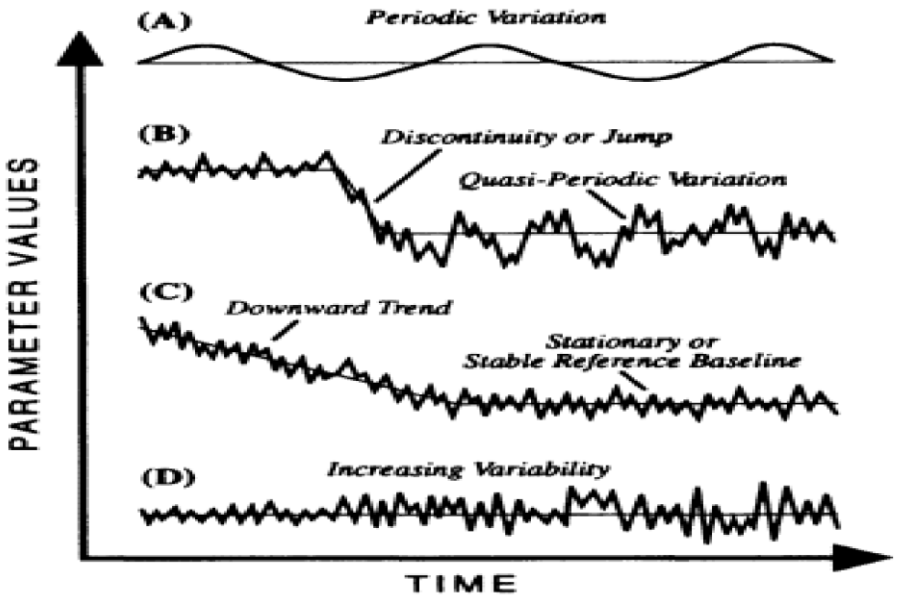

Figure 2.1: Types of climate variations

a) Periodic change: This is as shown in Figure 2.1 it occurs in form of periodic cycles. The length of the cycles corresponds to the time scale adopted for the variability study that can either be daily, annual, decadal or longer time scales.

b) The climate may undergo a sudden shift from its current state to another state, maybe one characterized by significantly colder or warmer conditions as shown in Figure 2.1.

c) The climate may also undergo a steady change until a stable state is reached, for instant, steady warming or cooling as shown in Figure 2.1.

d) Another common pattern is where the climate maintains what appears to be a steady state when characterized by a specific variable e.g. Mean annual temperature, but variations in other measures e.g. seasonal temperature, diurnal range of temperature indicates that significant change has taken place as shown by Fu *et al.*, (2009) on Figure 2.1.

2.4 Temperatures variability

2.4.1 Global variability

It is estimated that global temperature has increased by 0.6^{o}C since the 19th century (KNMI. 2006). In the recent decades (1950 – 1993), the increase in temperatures has involved a faster rise in daily minimum (0.2^{0}C / decade) than in daily maximum (0.1^{0}C / decade) in many continental regions. This has led to a decrease in diurnal temperature range (-0.1 ^{0}C / decade trend) in many parts of the world (Parry, 2007). This is a rate higher than for the mean temperatures for the entire 20th century, indicating very strong warming in recent decades. The challenge with these ranges is that they were done for only 57% of the global surface and hence may not accurately reflect the global trend. However, with more GCM models in the market this is likely to change (Westmacott & Burn, 1997).

2.4.2 Regional variability

According to Lins and Slack (1999), temperatures have increased almost everywhere with the exception of eastern Canada, small areas of Eastern Europe and the middle east. The diurnal temperature range has decreased in most areas except over middle Canada, and parts of South Africa, south-west Asia, Europe and western tropical pacific islands. In New Zealand and central Europe, maximum and minimum temperatures have increased at similar rates. Other regions like India have experienced increased diurnal temperature range due to decrease in minimum temperatures (Lins and Slack, 1999). These different occurrences of variability across regions make the assumption of a global value insufficient for evaluation of impacts and planning of mitigation at local scale. This leads to the need of assessing variability even at local scale i.e. sub regions of the continental regions are generally adopted in such studies (Fu *et al.,* 2009).

2.5 Precipitation variability

Over the 20th century, the annual precipitation increased by between 7% and 12% for the zones 30^0N to 85^0N and by about 2% between 0^o to 55^oS (IPCC *et al.,* 2000). In the year 1998 the high latitudes (55°N and higher) of the Northern hemisphere had their wettest year on record and the mid-latitudes recorded precipitation totals exceeding the 1961 to 1990 mean every year since 1995 (Beven, 1989). Studies have shown that precipitation in Canada has increased by about 10% during the 20^{th} century. In china there has been a declining trend in total annual precipitation for the period 1950 to 2000 (Ndirangu *et al.,* 2009). Studies have shown multi-decadal variation in the Indian monsoonal rainfall, from 1906 to 1960 the rainfall increased and then decreased through 1974 and has continued to increase since then, western Mexico has experienced an increasingly erratic monsoonal rainfall since 1940s (Fu *et al.,* 2009). The driest period was in the 1980s. Southern Africa region has experienced significant decreases in precipitation since 1970s. Early 2000 have seen flood-producing rains in the eastern part of South Africa (Lukeman, 2003). From all this consideration, it is seen generally that there is an increasing trend in precipitation.

2.6 Climate variability impacts

Climate variability has several impacts (Hay et al., 2002). Bases on climate change projections made by IPCC, climate change increases the occurrence of droughts, floods and extreme rainfall events (IPCC, 2007). Recent studies show that cyclones intensity will increase with up to 10-20% due to climate variability. More El Niño like weather conditions are expected as a result of climate variability. All these will have an impact on crop agriculture, forestry, livestock and human life in general (van de Steeg *et al.,* 2009).

2.6.1 Assessment of climate variability effects

As presented by IPCC (2007), a set of four future climate scenarios to project emission gases and temperatures are paramount to addressing these unforeseen challenges. These scenarios are used by researchers and policy makers to assess potential future conditions and compare them to baseline conditions in the absence of climate change. As an example rainfall variability in Kenya affects agricultural production and the livelihoods of people, especially in the ASAL areas, like Makindu (John Walker Recha *et al.,* 2016). These scenarios can also be used to analyze adaptation scenarios to mitigate the negative effects of climate change.

2.6.2 Water resources under climate variability

Runoff is a key area in water resources and can be affected by environmental changes. It is also influenced by the changes in temperature and precipitation. Runoff being an important in water supplies dynamics has led to more and more research on the impacts of environmental changes on overflow. It is important to look at runoff as a little representation of precipitation. Its magnitude depends on temperature, dampness, solar intensity, vegetation, wind speed, and soil moisture. In this case, changes in runoff are not similar to changes in precipitation. Fredrick and Gleick (1999) were able to model effects of temperature and changes in precipitation on different stream bowls hence effectively investigating the effects of environmental change on water supplies. They found that by expanding temperature by $2^{o}C$ and reducing precipitation by 10%, the measure of runoff inside the Great Basin Rivers, Upper Colorado, Lower Colorado, and Colorado River will diminish by - 17% to - 28%, - 35%, - 56%, and - 40% (Miller, 1997) respectively.

In Kenya dry extremes are projected to be less severe than they used to be during September to December (Wambua *et al.* 2014). Despite this, the GCM does not give a good agreement on the projected changes in dry extremes during the months of March to May (KNMI, 2006; Thornton *et al*., 2006). The wet extremes also known as short and long rains are experienced from September to December and March to May rainy season respectively. In the northern regions, the dry extremes are projected to be less severe during September to December (KNMI, 2006). Despite this, the GCM model fails to show a good agreement in the projected changes of the dry extremes which are expected from March to May (Thornton *et al.* 2006).

According to KNMI (2006), on average, the projected variations in wettest events occur once in every 10 years. It is important to take note of the fact that the existing climate models underestimate the strength of long rains in current climate. This limits the confidence of the projections (KNMI, 2006; Thornton *et al.* 2006). There are 112 models which were used by KNMI (2006). Through use of these models, KNMI investigated on the precipitation changes using the runs forced through Special Report Emission Scenario (SRES) A1B scenario (KNMI, 2006). According to Osbahr and Viner (2006), increases in temperatures have a significant impact on water availability. The increases are expected to exacerbate drought conditions which are experienced regularly. Rainfall in Kenya is unpredictable and has a tendency to fall heavily in short periods. This is likely to cause problems through increased occurrences of heavy rainfall periods as well as flooding (Osbahr and Viner, 2006).

2.7 Climate variability and change scenarios

Based on state of the Special Report on Emissions Scenarios (SRES) (IPCC, 2000), climate change scenarios are not the prediction or forecast of the future but rather they are potential future scenarios and each of scenario represents a way in which the future might unfold. There is little information on climate change available for East Africa at both country and local scale. In Kenya, rainfall projections are inconsistent as evidenced by a range of models and scenarios which shows increases and decreases in total precipitation (Osbahr and Viner, 2006).

According to IPCC (2007), a climate variability scenario is the estimation of future resource availability factoring in the estimation of the implications of climate change or variability for water stress. The scenarios describe future demographic conditions, environmental conditions, social conditions, economic conditions, technologies, and policies. The four scenarios described by the IPCC (2000) are Al, A2, B1 and B2 Scenarios.

2.7.1 A1 Scenario**:**

"This scenario describes a world with a very rapid economic growth and a global population that attains its peaks in mid-century. The population declines thereafter with new and more efficient technologies being rapidly introduced. Major underlying themes are convergence among regions, capacity building and increased cultural and social interactions, with a substantial reduction in regional differences in per capita income. The three A1 groups are distinguished by their technological emphasis: fossil-intensive (A1FI), non-fossil energy sources (A1T) or a balance across all sources (A1B)."

2.7.2 A2 Scenario:

"The A2 scenario and scenario is based on describes a very heterogeneous world. The main theme is self-reliance and preservation of local identities. Fertility patterns across regions converge very slowly, which results in continuously increasing population. Economic development is regionally oriented and per capita economic growth and technological change more fragmented and slower than other storylines."

2.7.3 B1 Scenario:

"This scenario shows a convergent world with the same low population growth as in the A1 scenario, but with a fast change in economic structures toward a service and information economy, with reductions in material intensity and the introduction of clean and resource-efficient technologies. The emphasis is on global to economic, social and environmental sustainability which includes improved equity, but without additional climate initiatives."

2.7.4 B2 Scenario:

"The B2 storyline and scenario family is based on a world in which the emphasis is on local solutions to economic, social and environmental sustainability. It is a world with an increasing population, at a rate lower than A2. The level of economic development is intermediate, and there is less rapid and more diverse technological change compared to B1 and A1 storylines. It is important to note that while the scenario is also oriented towards environmental protection and social equity, it focuses on local and regional levels."

These scenarios are as summarized in Table 2.1.

Table 2.1 Scenarios to be adopted

	SCENARIO 1 (low)	**SCENARIO 2 (high)**
Temperature (increase in degrees)	0.2	0.5
Rainfall (%increase during wet months)	5	20
Rainfall (% decrease during dry months)	5	10

2.7.5 Generation Global Climate Model (GCM)

GCM is widely applied for weather forecasting, understanding the climate and projecting climate change. Mathematical models are used to simulate the present climate and predict future climate while considering impacts of greenhouse gases and aerosols. As they are based on physical laws and physically based empirical relationships, GCMs are, therefore, the only tools that estimate changes in climate due to increased greenhouse gases for a large number of climate variables in a physically consistent manner (Watson *et al.*, 2001). Praveen Kumar *et al.* (2012) demonstrated that GCMs are very important in climate variability studies were they found that they were very reliable in predicting India's rainfall. This was achieved through simulation of monsoon rainfall at a 95% confidence level.

2.8 Runoff under climate variability

By far the highest frequency of hydrological studies into the effects of climate variability has focused on potential changes on river flow (Maidment, 1992). The distinction between "stream flow" and "runoff" may well be vague, however in general terms stream flow is water within a river channel, usually expressed to be the rate of flow past a point typically in $m^3 s^{-1}$, whereas runoff is truly the quantity of precipitation that does not evaporate, usually expressed as an equivalent depth of water along the area of the catchment. A good link between them is that runoff can easily be considered stream flow divided by catchment area, although in dry areas this doesn't necessarily hold because runoff generated in a single area of the catchment may infiltrate before reaching a channel and becoming stream flow. Over short durations, the amount of water leaving a catchment outlet usually is expressed as stream flow; over durations of a month or more, it usually is expressed as runoff (Maidment, 1992).

Lvovitch (1972) suggests that the distribution of runoff per continent shows some interesting patterns as stipulated in Table 2.1. Areas having the most runoff are the ones with high rates of precipitation and low rates of evaporation.

Table 2.1: Continental run-off values

Continent	Runoff Per Unit Area (mm per yr.)
Europe	300
Asia	286
Africa	139
North and Central America	265

2.9 Trends in observed stream flow

Since the second assessment report, there have been many notable hydrological events-including floods and droughts-and therefore many studies into possible trends in hydrological data (Wambua *et al.* 2014). In general, the patterns found are consistent with those identified for precipitation: Runoff tends to increase where precipitation has increased and decrease where it has fallen over the past few years (Lins and Slack, 1999). The variability of runoff and water resources is particularly higher for drier climates, e.g., a higher percent change in runoff resulting from a small change in precipitation and temperature in arid or semiarid regions (Fu *et al.*, 2009). It is very important for water resources managers to figure out and prepare to tackle the effects of global climatic variability on the changes of hydrological cycles and stream flow regimes. The better understanding toward the relationship between global climatic change/variability, anthropogenic activities and the water resources availability in addition to its withdrawal and exploit, will allow water resources managers to make more rational decisions on water allocation and regulation (Pacini and Harper, 1998).

2.10 Hydrological models

The rainfall runoff models classifications are based on the input parameters together with the physical principles applied (Moradkhani and Sorooshian, 2008). This leads to classification of models as lumped and distributed based on the parameters which are function of both time and space. They are also classified as deterministic and stochastic models according to other criteria. The deterministic models can only give same output based on a given set of input (Refsgaard,

1996). This is contrary to stochastic models which give varying values of outputs for a given single set of inputs (Moradkhani and Sorooshian, 2008).

Moradkhani and Sorooshian (2008) assert that the entire river based output is considered as a single unit. In this case, spatial variability is disregarded and outputs are generated without considering the spatial processes. In this case, a distributed model can be used in making predictions that are distributed in space. This is realized by dividing the entire catchment into small units which in most cases are square cells or triangulated irregular network. In this case, the parameters, inputs and outputs vary in a spatial manner. Based on time factor, it is possible to classify the models as static or dynamic (Osbahr and Viner 2006). Static model excludes time unlike the dynamic model. According to Sorooshian *et al*. (2008), the models can be classified as event based or continuous. It is important to note that the former can only produce output in specific time intervals unlike the latter which has a continuous output. The most vital classifications are empirical model, conceptual models and physically based models (Osbahr and Viner 2006).

2.10.1 Empirical models

Empirical model also referred to as Metric model is an observation based model which only takes information from the existing data without taking consideration for the features and processes of hydrological models (Osbahr and Viner 2006). The models are also known as data driven models. They involve use of mathematical equations which are derived from the concurrent input and output time series and not from the physical processes of catchment (Sorooshian *et al.* 2008). These types of models are only valid when used within the boundaries. Regression and correlation are used by the statistically based methods and helps in finding the

existing relationship between inputs and outputs. Some of the machine learning techniques used in hydroinformatic methods are neural network and fuzzy regression (Moradkhani and Sorooshian, 2008).

2.10.2 Conceptual methods

Parametric models which are also referred to as parametric models are used in describing all hydrological processes. This consists of a number of interconnected reservoirs which are used as a representation of the physical elements in a catchment. The reservoirs are recharged by the rainfall, infiltration, and percolations and are emptied through evaporation, runoff and drainage among others (Abbott *et al.* 1986 a, b). Use of semi empirical equations in this method and model is not only accessed from field data but also from calibration. Large number of meteorological and hydrological data is required for calibration. Calibration includes use of curve fitting making interpretation difficult hence effects of land use cannot be predicted accurately (Osbahr and Viner 2006). Many of the conceptual models are developed with varying degrees of complexity. Stanford Watershed Model IV (SWM) is the first major conceptual model developed by Crawford and Linsley in 1966 with 16 to 20 parameters.

2.10.3 Physically based model

This model is a representation of a real problem mathematically. Physical based model is also known as a mechanistic model and includes principles of physical processes (Refsgaard, 1996). The model uses state variables which are measurable and are functions of time and space. Through use of finite differential equations, it is possible to represent hydrological processes of water. The model does not require use of extensive hydrological and meteorological data during calibration (Abbott *et al.* 1986a, b). Despite this, there is evaluation of large number of

parameters which describes the physical characteristics of the required catchment (Abbott *et al.*1986a). Through this method, a huge amount of data which includes soil moisture, water depth, topology and the dimensions of river network are required (Refsgaard, 1996). Physical model has the ability to overcome a lot of defects which are in the other two models since it uses parameters with physical interpretation. The model can provide a large amount of information even outside the boundary and can be used in a wide range of situations. SHE/ MIKE SHE model is an example (Abbott *et al.* 1986a, b).

2.11 Rainfall – Runoff models

2.11.1 USDA HL-74 watershed model

This is a continuous model intended specifically for small Agricultural watershed (ASCE, 1999). The SWBM is continuous model which is suitable for an ASAL Watersheds but its use is constrained by availability of stream flow data, measured for at least five years (Luijten, 1999). However, this model could not be applicable in the assessment of climate variability effects on Thika catchment because the catchment does not fall in ASAL area.

2.11.2 HEC-1Model

The hydrologic modelling system (HEC-1) model is a continuous simulation model developed by US corps of Engineers for planning design and operation of water project in the Columbia River Basin (HEC, 2000). HEC-1 is a single event lumped parameter model frequently used to develop hydrographs for project design rather than climate studies (Singh, 1995).

2.11.3 VIC model

Also referred to as Variable Infiltration Capacity model, it is a semi distributed grid based hydrology model which uses both energy and water balance equations. The main inputs are precipitation; minimum and maximum daily temperature and wind speed and allows many land cover types within each model grid (Gao, 2010). The processes like infiltration, runoff and base flow are based on various empirical relations. Surface runoff is generated by infiltration excess runoff (Hortonian flow) and saturation excess runoff (Dunne flow) (Moradkhani and Sorooshian, 2008). VIC simulates saturation excess runoff by considering soil heterogeneity and precipitation (Linsley, 1972). It consists of three layers where the top layer allows quick soil evaporation, middle layer represent dynamic response of soil to rainfall events and lower layer is used to characterize behavior of soil moisture (Moradkhani and Sorooshian, 2008).

Improvised VIC model has included both infiltration excess runoff and saturation excess runoff and also the effects of variability of soil heterogeneity on surface runoff characteristics. It can deal with the dynamics of surface and ground water interactions and calculate ground water table (Gao, 2010) and can be applied in cold climate. The model has nowadays been applied to a number of river basins and helps in predicting climate and land cover changes over the study area (J. Wei *et al.*, 2016).

2.11.4 Stanford Watershed Model

Stanford watershed model developed by Stanford faculty members Ray Linsley, Joseph B. Franzini, and John K. Vennard in 19th century is a continuous, distributed model is intended for application into watershed of all sizes. Primary data input includes the hourly and daily precipitation and daily maximum and minimum temperatures. According to Ray (1975), the

greatest drawback with the model is in its incapacity to take in various climate scenarios when simulating.

2.11.5 HYSIM Model

HYSIM is a theoretical rainfall runoff-model, which utilizes precipitation and potential evaporation information to mimic river flow parameters. The model has been used in Scotland among other places to study climate variability effects (Scottish Water, 2009).

2.12 The HYSIM conceptual rainfall-runoff model

2.12.1 Model Overview

HYSIM was authored by Manley (1993) as a commercial package. The model origin can be traced back to the 1970s. Despite this, the commercial PC version of HYSIM was coded in Visual Basic for DOS by Microsoft and released in 1992. At the point of model development, the author had the essential prerequisite that the parameters of the model ought to be physically significant (Manley, 1978). This information on HYSIM is prevalently based on the data distributed in the user and technical guides (Manley 1992a, 1992b). It was created by the Water Resource Associates (WRA). WRA are a group of experts in water assets, water quality, hydrology, groundwater hydrology and flooding. Their customers include probably the most critical water administration bodies in Europe such as the European Union, United Kingdom Environmental Agency, National Power, French government, British Waterways and SNIFFER (Manley, 1978).

According to Manley (1993), HYSIM is a theoretical rainfall runoff-model, which utilizes precipitation and potential evaporation information to mimic river flow parameters for hydrology and hydraulics that characterize the river basin and channels realistically. Despite being spatially

lumped and hydrological conceptual in nature, HYSIM model has a number of dimensions that can be determined from physical reality. HYSIM model is based on two sub-routines; the first routine simulates catchment hydrology and the second simulates channel (Manley, 1978).

The combined program with other models is viewed to be among the techniques for estimation of yield (Scottish Water, 2009) and enhances past estimations of yield. This combination of the Aquator software with the rainfall-runoff model is currently being used in England while the Hydrologic Resource Center reservoir resource Simulator (HEC-ResSim), developed their model incorporating HYSIM into it (US Army Corps of Engineers, 2011). HYSIM is based on two IBM mathematical formula translating system (FORTRAN) (Manley, 1978). At first, the model processes both the hydrology and hydraulics of a catchment independently. When the model is run, the parameters govern the limits and the rates of exchange between every store through mathematical equations hence the transfer process.

2.12.2 The Structure of HYSIM

HYSIM can be connected to single or various sub-catchments, each of which ought to be homogeneous regarding the soil structure. The model requires an input of five particular data types; of which none are compulsory. These are:

i. Catchment average precipitation time series;
ii. Catchment normal potential evapotranspiration;
iii. Catchment normal potential melt rate for snow;
iv. Net emanating/surface water abstraction rate;
v. Total groundwater abstraction rate.

The time venture for this information can be monthly, daily or sub-daily despite the fact that there is an option of using data with varying time steps. The model has been coded in a way that the water driven and hydrological parts can likewise be kept running on various time steps (Manley, 1978).

2.12.2.1 Snow and interception stores

If the precipitation is snow (as characterized in the input data), it enters a semi - limitless store. In the event that there is snow storage at time step I the outflow is equivalent to the input melt rate within every time step. The interception store represents detainment of water on vegetation. The limit of the interception store (c_i) has a greatest limit characterized by the maximum depth of the store (I_{max}) and the impermeable part of the catchment as presented in Equation 2.1:

$$Ci = Imax \times \frac{1-\text{IMPERMEABLE AREA}}{\text{TOTAL AREA}} \quad (2.1)$$

The store gets water from precipitation and snow melt (if any) and loses water by dissipation, which happens at the potential rate. Excess precipitation (EP) from interception store is divided between the upper soil horizon and minor channel storage by partial degree of the impermeable region of the catchment.

2.12.2.2 Soil moisture stores

Soil moisture comprises of two stores; the Upper Soil Horizon (USH) and the Lower Soil Horizon (LSH). The USH represents moisture held in the top soil (the A moisture horizon) whilst the LSH represents moisture beneath the USH. The USH has a finite limit given by:

$$C_{USH} = D_{USH} \times F_{USH} \quad (2.2)$$

Where D is the depth of the zone (mm) and F is the mean porosity of the zone.

The maximum rate at which the store can acknowledge EP is controlled by an estimate to the Philip's invasion mathematical statement (Philip, 1957). Manley (1977) showed that Philip's mathematical statement can be approximated by:

$$x = (2K_1P.t)^{0.5} + k_1t \quad (2.3)$$

Where

x is the separation voyaged downwards by the wetting front (mm),

k, is the saturated permeability at the top of the horizon (mm/hr.),

t is the duration of the time step and

P is the capillary suction (mm. H_20). This relationship encourages the count of the most extreme, or potential, penetration rate over the time step. EP steered to the USH in excess of this restricting rate is directed to the minor channels store as overland flow. It has been demonstrated that P can be expressed as:

$$P = \frac{P_b}{S_e^{\frac{1}{\gamma}}} \quad (2.4)$$

Where P_b is the percolating weight (mm/hr),

y is the pore size dispersion file and

S_e the powerful immersion which is characterized as:

$$S_e = \frac{m - S_r}{1.0 - S_r} \quad (2.5)$$

Where *m* is the saturation toward the start of the time step and S_r is the remaining immersion which is the base immersion that can be obtained by de-watering the soil under expanding suction. Evapotranspiration happens from the USH at the potential rate (less any loss from the interception storage) if P is under 15 atmospheres (Lukeman, 2003). In the event that P is more

prominent than 15 atmospheres dissipation happens at a rate decreased in proportion to the remaining depth of water storage.

The next exchange of moisture is by means of interflow. As demonstrated by Manley (1978) in Equation 2.6, conceptualization of bury stream depends on the Brookes and Corey observational model for the viable porousness of permeable media. Interflow is figured utilizing:

$$\text{Interflow} = \text{Rfac1}(S_e)^{\frac{(2+3\gamma)}{\gamma}} \tag{2.6}$$

Where Rfac1 is characterized as the interflow from the USH at extreme saturation. The power function of S_e is used to balance Rfac1 when the saturation is lower than the extreme. This reflects that, conceptually, lateral porousness will be less when the soils are not completely saturated. The last exchange of moisture is by percolation from the USH to the LSH, where permeation is estimated in an analogous approach to inter flow utilizing:

$$\text{Percolation} = K_b(S_e)^{\frac{(2+3\gamma)}{\gamma}} \tag{2.7}$$

Where K_b is saturated porousness at the horizon limit. By consolidating the mathematical statements for Interflow and permeation the change in storage can be evaluated through:

$$\frac{ds}{dt} = I - (\text{Rfac1} + K_b)S_e^{\frac{(2+3\gamma)}{\gamma}} \tag{2.8}$$

Where I is the net inflow rate.

This common differential comparison can't be solved unequivocally as the estimation of S_e is a component of the water in the storage. However, a scientific estimate is found if the inflow over a period step is steady and the aggregate change away over a period step is little in contrast with the total depth of water at the beginning of the time step. This last suspicion implies that Se can be taken as being consistent over the time step being considered. Inside HYSIM the adjustment

away is obliged to lie between an upper and lower limit. Upper limit is determined by the storage capacity at which the rate of output is equivalent to the rate of inflow. Lower limit is obtained from setting 1=0. It is not clear whether this rough arrangement guarantees that mass is preserved.

The permeation from the USH forms the input to the lower soil horizon (LSH). The LSH is configured similarly to the USH where the penetration of percolation is controlled by the capacity of the LSH to acknowledge percolation from the USH. Percolation in excess of the penetration limit is directed to the minor channels store. Loss from the LSH through inter flow stream and permeation to the groundwater is controlled by similar equations to the USH. Evaporation potential that is not met by the USH is met from the LSH, subject to the same suction weight requirement that operated in USH (Lukeman, 2003).

2.12.2.3 The Groundwater Store

The groundwater store is subdivided into two infinite direct supplies; the transitional groundwater and deep groundwater stores. The transitional groundwater store gets percolation from the LSH, represents the primary phase of groundwater storage where direct release to surface waters might happen by means of fissure flow (Dooge, 1973). The outflow from the transitional groundwater store is partitioned between the minor channels store and the deep groundwater store. The deep groundwater store releases to the minor channels. It is from this groundwater store that ground water deliberations can be made. The function characterizing the surge, q, from a linear reservoir is given by:

$$q = \frac{1}{k}s \qquad (2.9)$$

Where

s is the volume of water in storage (Cubic Meters) and

k is a constant (with units of time).

This explicit formulation neglects that within a time step the instantaneous value of s is dependent on the function of the outflow q. combining this power equation with the equation of continuity gives:

$$\frac{ds}{dt} = u - q \tag{2.10}$$

Where u is the inflow over the time period yields:

$$\frac{dq}{dt} = \frac{1}{k}.q.(u - q) \tag{2.11}$$

Which is the linear representation of the Horton-Izzard model (Dooge, 1973).

2.12.2.4 The Minor Channels Store and Hydraulic Routing

The minor channels store represents flow routing in minor streams, trench and, if the catchment is saturated, ephemeral streams. This store uses a triangular Instantaneous Unit Hydrograph (IUH), with the time base equivalent to 2.5 times the peak time. Time to peak is assessed utilizing the Flood Studies Report mathematical statement (NERC, 1975) given as:

$$T_p = 2.8\left(\frac{L}{\sqrt{S}}\right)^{0.47} \tag{2.12}$$

Where T_p is an ideal peak time, L is the stream length (km) and S is the stream slope (m/km).

The time base of the IUH reaction to influent volume, V, = $q_i.t$, in time step (t) will be calculated by:

$$T_l = \tau\left(\frac{L}{\sqrt{S}}\right)^{0.47} \tag{2.13}$$

Where

T_L is the time base of hydrograph, and

q_t is equivalent to zero at x = 0 and

$\tau = T_L$ The maximum flow rate (q_{max}) happens at T_p and is given by:

$$q_{max} = \frac{q_t \cdot t}{1.25\ T_p} \quad (2.14)$$

The "main" stream inside HYSIM is represented as a number of hydrology homogenous reach. Velocity of water along a reach is portrayed by the kinematic wave estimation to the Saint Venant's comparisons:

$$V_w = \frac{\Delta Q}{\Delta A} \quad (2.15)$$

Where ΔQ and ΔA are the incremental changes in speed along the scope and hydraulic cross-sectional zone. The kinematic wave estimate is utilized as the Saint Venant mathematical statements can't be tackled unequivocally. An experimental model is utilized within HYSIM for assessing cross-sectional area. The estimate considers that most channels lie between the two extremes of a rectangular channel and triangular channel. The form of this approximation is as follows:

$$Q = CA^{1.5} \quad (2.16)$$

Where C is a coefficient of proportionality.

If bank flows may occur then Manley (1978) advises the user to develop site specific coefficients which HYSIM will use under these conditions. Manley (1978), also advises the development of two such sets; the first for use when the flood plain is filling and the second when the flood plain is full. HYSIM has facilities for using the hydraulic sub model to link together a number of sub

catchment models in series, thus enabling the model to be used in a semi-dispersed mode (Manley, 1978).

2.12.3 Model Parameters

Parameters modifications are split into three segments inside HYSIM, these are information, basic and advanced. According to Jacobs (2010) standard calibration technique, which is based on the HYSIM User Manual (Manley, 2006), the information specific and advanced hydraulic parameters stay at their default values. The essential hydrological parameters that are changed are outlined at their default values in Table 2.2.

Table 2.2: Model Parameters

Parameters	Description	Default
Interception storage (mm)	Moisture storage before infiltration	2.00
Impermeable Proportion	Portion of the catchment where water cannot penetrate	0.02
Time to peak (hrs.)	time interval from the start of the resulting hydro graph	2.00
Rooting Depth (mm)	the depth of soil from which plant roots take up water, or the depth of soil to which roots reach	1000.00
Pore size distribution index	measure of the void (i.e."empty") spaces in a material	0.15
Permeability (horizon boundary) (mm/hr.)	the state or quality of a material or membrane that causes it to allow liquids or gases to pass through	10.00

	it	
Permeability (base lower) (mm/hr.)	the state or quality of a material or membrane that causes it to allow liquids or gases to pass through it	10.00
Interflow (upper) (mm/hr.)	Movement of water between layers	10.00
Interflow (lower) (mm/hr.)	Movement of water between layers	10.00
Precipitation factor	Weighting factor for precipitation	1.00
PET factor	sum of evaporation and plant transpiration from the Earth's land	1.00
Catchment Area (sq. km)	Catchment Area	1.00

2.12.4 Previous application of HYSIM

According to CDI (2010), a successful implementation of HYSIM was in Yeşilirmak basin in Turkey in a drainage area of around 36,000 km^2 and flowing into Black Sea. The study was aimed at developing an understanding of the water balance in the basin and also examine the potential effects of climate change on the basin. To get the initial appraisal of the likely impacts of climate change, the simulated flow for the period 1980 to 1999 was compared with simulated flow for projected values for the period 2080 to 2099 (CDI, 2010). This is a hundred years in future relative to the observed period. Through the model, it was observed that the main effect of climate change to the basin was a reduction in spring flows. The results made it vital for the policy planners to think of a need for reservoir storage in the basin (CDI, 2015). In the Thika basin the model basically evaluates the climate variability effects on stream flows hence acting as a decision support tool to the planners.

2.13 Trend Analysis

This method usually employs testing of trends of the times series of the climatic data over time. Trend detection can be done by both analytical and graphical methods (Lins and Slack, 1999; Gocic and Trajkovic, 2012). The graphical methods involve the fitting of a trend line to a time series of the data. This method has the advantage of being visual, for instance, if a trend actually exists it can be seen visually and at times its magnitude can be appreciated from the slope of the trend line. However, this method is limited in that if the trend is too slight it may not be easily discernible and also the actual magnitude of the change cannot be accurately determined (Lins and Slack, 1999). Analytical methods have the advantage of revealing even the slightest changes and also the magnitude of the change. There are various methods used for trend detection depending especially on the nature of the data distribution. The broad categories are parametric and non-parametric methods (Lins and Slack, 1999).

2.13.1 Mann-Kendall's trend test's

The Mann-Kendall trend test is a non-parametric test used to detect trend in time series data. By the virtue of it being non-parametric, it does not require data to be of any particular distribution, it also has a high asymptotic efficiency (Hamed, 2008). The test statistic Z for a particular period will be estimated according to Fu *et al.* (2009) as follows:

$$\begin{cases} \frac{S-1}{(\mathrm{var}(s))^{0.5}}, & \text{if } s > 0 \\ \frac{S+1}{(\mathrm{var}(s))^{0.5}}, & \text{if } s=0 \\ & \text{if } s < 0 \end{cases} \qquad (2.17)$$

$$\mathrm{Var}(s) = (n(n-1)(2n+5) - \sum_t t(t-1)(2t+5)j/18 \quad (2.18)$$

$$s = \sum_{k=1}^{n-1} \cdot \sum_{j=k+1}^{n-1} \mathrm{sgn}(Xj - Xk) \quad (2.19)$$

Where

X is the variable, a sample of n independent and identically distributed random variables (e.g. Monthly precipitation or temperature) it is the extent of any given tie.

For testing the null hypothesis, H_o, meaning no significance trend, against H_1 significant upward trend, H_o is rejected if $Z > Z_{1-\alpha}$. Testing for significant downward trend H_2, reject H_o if $Z < 0$ and the absolute value of $Z > Z_{1-\alpha}$ (Fu *et al.*, 2009).

According to (Barnett, 1983, 1991; Casella and Berger, 1990), the choice used for a significant level (α) is completely arbitrary. Another way to carry out the test for hypothesis is through comparing the p-value of the sample test statistic with a significance level(α). In this case, the p-level of the sample test is the lowest level of significance where null hypothesis (H_0) can be rejected. The p-value is compared against actual significance level of the test and if it is smaller, results are taken as significant. If the null hypothesis is rejected at 5% significance level, it is reported as "$p<0.05$". Thus, the smaller the value is, the more convincing it becomes to reject the null hypothesis. This is rejection of the null hypothesis through use of strength of evidence rather than simply making conclusions "Reject H_0" or "Do not reject H_0". The p-value is very important in evaluation and interpretation of the findings. This makes it possible for the researchers to set their own level of significance. It also makes it possible to reject or accept null hypothesis based on their criterion instead of using fixed level of significance.

2.13.2 The Sen's slope for trend magnitude

The Mann Kendall trend test merely indicates the presence of trend but shows no indication of the magnitude of the trend. The Sen's slope is a formula that is used to measure the magnitude of the trend by estimating the slope of the assumed linear trend (Gocic and Trajkovic, 2012). When the data time series depicts a linear trend, a true slope can be estimated through use of a simple nonparametric procedure given by Sen (1968). The Sen's slope estimator denoted by, b, is determined using Equation. 2.20.

$$b = \text{median}\left(\frac{x_j - x_i}{j-1}\right) \quad \forall i < j \qquad 2.20$$

Where x_j and x_i are two generic sequential data values of a variable.

For a time series of annual values, b represents the annual increment under the hypothesis of a linear trend. The b estimator approximates the true slope of the trend, which can slightly differ from the slope of the trend line obtained by linear regression. Hirsch *et al*. (1982) concluded that a lurking variable was unlikely to be affected by outliers since sens estimate is robust against these outliers.

2.14 Modeling

2.14.1 Importing data to the HYSIM format

This is an option found under Tools/Import to HYSIM/ASCII (TXT) to HYSIM. The process involves importing data from an original file to HYSIM. On opening the data file, one opens the details for the template and saves the template with an appropriate name (e.g. Thika Catchment). On clicking on run/import the imported data hence becomes visible.

The next step is checking the correctness, in particular, looking at the end of December and start of January to ensure that the values are not out of phase and if OK then it is saved (‘File/Save data). The process is repeated for the potential evaporation and flows. Manley (1993) suggested that the algorithm used for conversion is usually stable but this also means that if one encounters an error in the starting date, or in the template file, the output file will not be correct.

2.14.2 Model Calibration

Calibration involves adjusting the models parameters. This includes parameters such as PET factor, soil infiltration coefficients to come up with acceptable accuracy. Through model calibration, it becomes possible to have proper water management. The greatest problem faced in calibration is inconsistency. A model can only reproduce one event but cannot reproduce another. Calibration in this case is aimed at "Single parameter" optimisation whereas confirming that PET factor has been selected and that "maximum iterations" selected as 10. For a successful calibration, it is important to obtain an accurate mean flow through adjusting the PET factor. This is followed by selecting the "Extremes Error of Estimate". Multi-parameter options should be selected by the user and confirmed that the four parameters selected are permeability at lower horizon, permeability at the horizon boundary, interflow at the upper horizon and interflow at the lower horizon. The number of iterations is supposed to be confirmed to be 50. The model should run again without optimisation and thereafter plot the results (Manley, 1972). At this stage the results should be getting good and if they are not, then the calibration process should be repeated. Hydrological simulation involved two important exercises that must be carried out successfully. These are calibration and validation of the model (Refsgaard, 1996). According to Beven (1989), calibration exercise is used in determining the best parameters in modeling studies and which is vital in the being that parameters can only be found through the calibration exercise.

2.15 Sensitivity analysis

According to Richard H. McCuen (1973), sensitivity analysis is very important exercise on model validation as well as its calibration. Most parameters when subjected to this analysis reflect how useful they are to the model parameterization and hence their optimization through this technique. This technique has been used in the various models and has proved vital to model parameterization. Marinoé Gonzaga da Silva *et.al.* (2015) demonstrated that analysis helps identify parameters most sensitive to the basin characteristics. This helped determine those parameters which would improve simulation results by the model through the totals of square errors (SSE) between the observed and simulated flows.

CHAPTER THREE

METHODOLOGY

3.1 Study area

3.1.1 Location

Thika river catchment lies between latitude $36^0$35’ and 37^0 35’E and longitude 0’35’ and 1’ 10’S and encompasses Murang’a, Thika, Machakos and Nyandarua sub counties in Kenya as shown in Template 3.1.

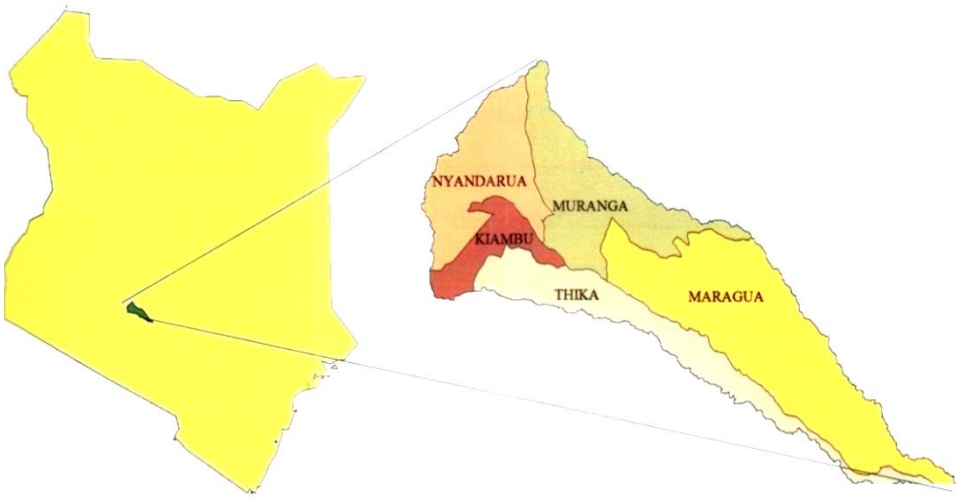

Template 3.1: River Thika Catchment

The catchment has an area of 867 km^2 and is approximately 40 km North West of the city of Nairobi (KMD, 2010) and it is part of the Tana catchment. Rivers Thika and Chania originate from the slopes of Nyandarua ridges and flow south eastwards for approximately 100 km before joining in Thika town to form the main Thika River. The river then flows for approximately 100km before joining River Tana. Within the larger catchment is Thika dam, located at a distance of about 80km north of Nairobi city. The dam catchment area features a fragile

ecosystem, owing to deforestation of Aberdare ranges, and a weak soil structure that is prone to landslides (Gathenya, 1999).

3.1.2 Topography

The land slopes generally in the eastern direction. Altitudes vary from 1525m a.m.s.l. at the catchment outlet and rises to 3,906m a.m.s.l at the headwaters of the Thika River. The average elevation is 1,700m a.m.s.l (KMD, 2010). Thika River which rises from the eastern Aberdare ranges drains the catchment. The river maintains a steep gradient in the upper reaches, but the gradient flattens out as it approaches the lower reaches of the catchment. The river flows south east wards to Thika town where it joins River Chania and forms the main Thika River about 100kms downstream (Gathenya, 1999). Thika River flows into River Tana on which the hydroelectric power dams are located. Two types of channels are defined within the catchment i.e. the main channel and tributary channels. In the Aberdare forested areas, runoff is minimized by the vegetation canopy unlike in the coffee zone where runoff is comparatively high (KMD, 2010).

3.1.3 Climate

The catchment is characterized by altitude dependent agro- climatic zones (humid to semi-arid). The rain distribution is bimodal with high peaks from March to May (long rains) and October to December (short rains). Annual rainfall varies from about 800mm at an altitude of about 1525m a.m.s.l to about 2200mm at an altitude of 2600m a.m.s.l (KMD, 2010). The annual potential evapotranspiration increases from about 1250mm at an altitude of 2400 a.m.s.l to about 1800mm at 1100m a.m.s.l (Gathenya, 1999).The temperature is high at the lowest altitude ranging from

25^0 C to 30^0 C but reduces to between 18^0 C and 20^0C towards the higher altitudes of 3500m a.m.s.l. (KMD, 2010).

3.1.4 Soils

The soils in the catchment vary with the parent material and also altitude. Deep into the forest the soils are well drained, very deep dark, silty clay loam, with humic top soil of mollic Andosols combined with well drained, dark reddish brown to very dark grayish brown, friable and slightly smeary clay, with a humic top soil of Ando curvicp haeozems (KMD, 2010). In the middle zone where small scale farming is mostly practiced the soils are extremely deep dark reddish brown to dark brown, friable and slightly smeary clay, with acidic humid topsoil generally of nit soils and sols type (Pacini and Harper, 1998).

3.1.5 Thika River Characteristics

River flows and gauges along the river were visited and their recorded flows over the years determined. This involved recording on minimum and maximum annual discharges from gauges and coming up with an average.

3.1.6 Parameterization variables

The parameterization of variables was carried out as shown on the table below. The parameters used are all listed in the Table 3.1.

Table 3.1: Parameterization variables

Parameters	Input File
Interception storage (mm)	Soil data file

Impermeable Proportion	Soil data file
Time to peak (hrs.)	Soil data file
Rooting Depth (mm)	Soil data file
Pore size distribution index	Soil data file
Permeability (horizon boundary) (mm/hr.)	Infiltration data file
Permeability (base lower) (mm/hr.)	Infiltration data file
Interflow (upper) (mm/hr.)	Infiltration data file
Interflow (lower) (mm/hr.)	Infiltration data file
Precipitation factor	Rainfall data file
PET factor	Rainfall data file
Catchment Area (sq. km)	Topography map file

3.2 Runoff Simulation

This involved simulation of changes in surface runoff considering the climate variability scenarios as suggested by IPCC and summarized in Table 2.1 earlier presented.

3.2.1 Base case and comparative period

The base period was between the years 1981 and 1995 while the period 2017 -2022 was chosen as an ideal comparative period and data obtained from the Second Generation Global Climate Model (GCM) for the period (Climate Data Information, 2015).

3.2.2 Weather data Input

This was the data required to simulate changes in runoff from the above climate variability scenarios. The input data required for this study included PET data, rainfall data, stream flow data and topological maps. This data was available from various sources which included IPCC weather data website, water resources management authority as well as Kenya Meteorological Department (KMD). The data was partitioned in two sets where 75% of it was used for testing and calibration and the rest 25% used for validation.

3.2.2.1 Rainfall Stations

Rainfall data was obtained from rainfall recording stations in and around the catchment. The data was in the form of daily mean rainfall for a period starting the year 1981 to 1996 for the calibration process and the period between 1960 to 1964 for the validation of the model. This was obtained from KMD stations in the catchment and then abstracted in its raw form from daily record sheets at the stations to excel sheets.

3.2.2.2 PET data

Potential evapotranspiration data was also required. However due to inability to obtain adequate and reliable PET data records, Subramanian et al. (1999) used Thornwaitte's equation to generate the data required. For this purpose, monthly mean temperatures as well as hours of sunshine were obtained from Water resources management authority that was used to generate the data. The PET data was divided into two sets the calibration set representing 75 percent of the data while the rest was used on validation.

3.2.2.3 Long term climatic data

Long term climatic data for Karuga, Kimakia, Thika stations was also obtained from the IPCC website. This data comprised of the long term means of the main climate change drivers i.e. rainfall and temperature. This data set for the period 1976 to 2006 was used for trend analysis.

3.2.2.4 Stream flow data

Discharge data (daily mean discharges) was required from the study area. This was obtained from gauging stations around the catchment. These were 4CB04 - Thika, 4CB05- Ndakaini and 4CB07 – Kimakia stations. This data was cleaned by an inbuilt function of the model that checked the missing data, infilled and also checked for its consistency respectively.

3.3 Model Calibration and validation

The HYSIM model was calibrated with daily stream flow data from years with the least number of missing values in both observed daily rainfall and stream flow. Calibration was done by manually adjusting the model calibration parameters. The direction and the rate of change of the parameters were guided by the results of the parameter sensitivity analysis as described by the user manual for the model. Visual and numerical methods were used to assess the goodness of fit between the simulated and the observed stream flow. In visual method the simulated and the observed stream flow was plotted on the same graph against time and compared visually. In numerical method observed and simulated stream flow was compared using the coefficient of determination (R^2) (Refsgaard, 1996). Rainfall, stream flow, and PET data from suitable period were used to validate the model. The simulated stream flow was compared to the observed. According to Refsgaard (1996), the model performance is evaluated using both visual and

statistical methods as in the calibration exercise. Assess and validate HYSIM model's ability to simulate surface runoff through use of rainfall, stream flow, and PET data from year 1981 to 1995 for 4CB04, 4CB05 and 4CB07 stations.

To effectively simulate flow, the Nash–Sutcliffe efficiency (NSE) (Nash and Sutcliffe, 1970); percent bias (PBIAS) (Gupta et al.,1999); and the mean absolute error (MAE) (Dawson and Wilby, 2001) were used to evaluate parameters behavior. The NSE evaluates the line of best fit between the observed flow against the simulated flow (Moriasi et al., 2007). An NSE value closer to 1 reflects a very good accuracy for the hysim model. PBIAS is expressed as a percentage between the simulated flow being more or less than the observed flow. + (-) PBIAS values reflects that the simulated flow exceeds (was below) the observed flow.

3.4 Sensitivity analysis of the model parameters

The parameters tested under this analysis were as outlined by Manley (1972). This was done using the default parameters initially and later adjusted to determine their sensitivity to the hydrological simulation. The parameters tested were precipitation factor, PET factor and rooting depth as suggested by Manley (1972). Marinoé Gonzaga da Silva *et al.* (2015) suggested the following procedure where an incremental addition to the parameters should be done followed by substitution by other values other than the default for a period not less than 6 months of the observed data. This was applied for the data for the period starting January 1960 to December 1963. Parameter sensitivity was calculated as the percentage difference between the simulated data and the observed data immediately after running the model as shown on equation 3.1.

$$\text{Sensitivity} = ((\text{Observed value} - \text{Simulated value})\% \qquad \text{Equation 3.1}$$

3.5 Trend Analysis

3.5.1 Mann Kendall's test

The non-parametric Mann Kendall's test was used to detect trends in precipitation and temperatures over the 30-year period. The data value was evaluated as part of an ordered time series. Each of the data value had to be compared with the subsequent data values. In instances where the data value obtained was higher than the later period value, an increment of 1 was added to statistic S. Also, when the data value from later period was lower than value which has been obtained earlier, a decrement of 1 to S was applied (Hamed, 2008). A significance level of 0.05 (5%) was used in this study as the level below which a significant trend can be observed. Effectively, in instances where Mann-Kendall test has a statistic above 1.96, the trend present in the data was said to be significant.

3.5.2 The Sen's Slope for Trend Magnitude

The Sen's slope formula was used to measure the magnitude of the trend in both temperature and precipitation by estimating the slope of the assumed linear trend. To get value of slope estimate (Q), the following formula as shown in Equation 3.1was used (Hamed, 2008).

$$Q_i = \frac{x_j - x_k}{j - k}, i = 1, 2, \ldots N, j > k \qquad (3.1)$$

Where:

Q_i is the slope

X denotes the variable

J, K are the indices

N is the data size

CHAPTER FOUR

RESULTS AND DISCUSSION

4.1 Study Area

4.1.1 Thika River Characteristics

Records of stream flow at for the period from 1960 to 2003 were readily available in digital form for the WRMA office. For the purposes of this study, three stream gauges were examined. The temporal coverage of the data at these gauges varied, and were operational at the same time. A summary of the stream gauges is as presented in Table 4.1.

Table 4.1: **Thika river characteristics**

Station	Annual Max Flow (m^3/sec)	Annual Min Flow (m^3/sec)	Annual Mean Flow (m^3/sec)	Monthly Min Flow (m^3/sec)	Monthly Max Flow (m^3/sec)	Monthly Mean Flow (m^3/sec)	First Date Available	Last Date Available
4CB04	21.9	1.1	4.2	1.1	6.2	4.1	01/01/1960	31/12/2003
4CB05	27.3	6.2	7.3	6.8	27.2	7.2	01/01/1960	03/08/1998
4CB07	19.5	2.8	10.2	2.8	20.3	10.8	01/01/1960	15/10/2000

From the results presented in Table 4.1, gauge 4CB04 had a maximum annual flow of 21.9m^3 and minimum annual flow of 1.03m^3 which gave an average annual flow of 4.27m^3. Gauge 4CB05 showed a maximum annual flow of 27.3m^3 and a minimum annual flow of 6.27m^3 giving an average annual flow of 7.36m^3. Lastly, Gauge 4CB07 gave a maximum annual flow of 19.5m^3 and a minimum annual flow of 2.86m^3 which gave an average annual flow of 10.26m^3. This dataset was then to be used as an input to rainfall runoff modelling software.

4.1.2 Rainfall Stations

Rainfall data was one of the inputs for the hydrological model. The rainfall data used for Thika catchment in this study was obtained from different sources and had varying quality and coverage over times. These sources were KMD and the IPCC website (IPCC,2007). Data availability is shown on Table 4.2.

Table 4.2: Rainfall Stations

Station	Annual Max (mm)	Annual Min (mm)	Annual Mean (mm)	Monthly Min (mm)	Monthly Max (mm)	Monthly Mean (mm)	Data Set Period
9036220	3996	0	772	0	1656	423	1976 - 2006
9036233	4023	0	759	0	1423	526	1976 - 2006
9137048	3026	10	765	10	1296	624	1976 - 2006

The yearly rainfall data was available in almost every station. The stations which had some missing data were Karuga farm – station ID 9036220 in 1987 and Kimakia - station ID 9036233 in 1983. The mean annual rainfall from the three stations was 772mm in Karuga farm, 759mm in Kimakia and 765 in Thika. The rainfall analysis started by carrying out thorough quality control of the data from KMD. Quality control in this case was used in correcting errors in the data and filling gaps where appropriate.

4.1.3 Data cleaning results

The years chosen for use had less gaps in the flow records. The model infilled the gaps using an inbuilt model function with a default value of -999.9.

4.2 Sensitivity analysis results

This was performed on the three model parameters namely precipitation factor, PET factor and also the rooting depth. An increment in the precipitation factor showed an increment (decrement) in the simulated flows while the PET and rooting depth increment (decrement) showed no or minimal effects on the simulated flow for the period between January 1960 and December 1963.

4.3 HYSIM model calibration and validation

4.3.1 HYSIM calibration for the period 1981 - 1995

The objective of model calibration was to minimize the error between observed and simulated water levels. This was done through the adjustment of the model parameters. Initial parameters before and after calibrations are presented in Table 4.3.

Table 4.3: HYSIM Parameterization variables

Parameters	Default	Calibrated value
Interception storage (mm)	2.00	20.00
Impermeable Proportion	0.02	0.02
Time to peak (hrs.)	2.00	2.00
Rooting Depth (mm)	1000.00	2000.00
Pore size distribution index	0.15	0.16
Permeability (horizon boundary) (mm/hr.)	10.00	11.03
Permeability (base lower)	10.00	10.98

(mm/hr.)		
Interflow (upper) (mm/hr.)	10.00	9.42
Interflow (lower) (mm/hr.)	10.00	9.56
Precipitation factor	1.00	1.04
PET factor	1.00	5.34
Catchment Area (sq. km)	1.00	897

The HYSIM model was calibrated using stream flow data from 1981-1995 for 4CB04, 4CB05 and 4CB07 in batches of 5 years and an average coefficient of determination (R^2) obtained as 0.923 as shown in Figure 4.1 and visually on Figure 4.2. The value of R^2 obtained corresponds to the results by Murphy and Charlton (2006) who obtained a value between 0.7 and 0.85.

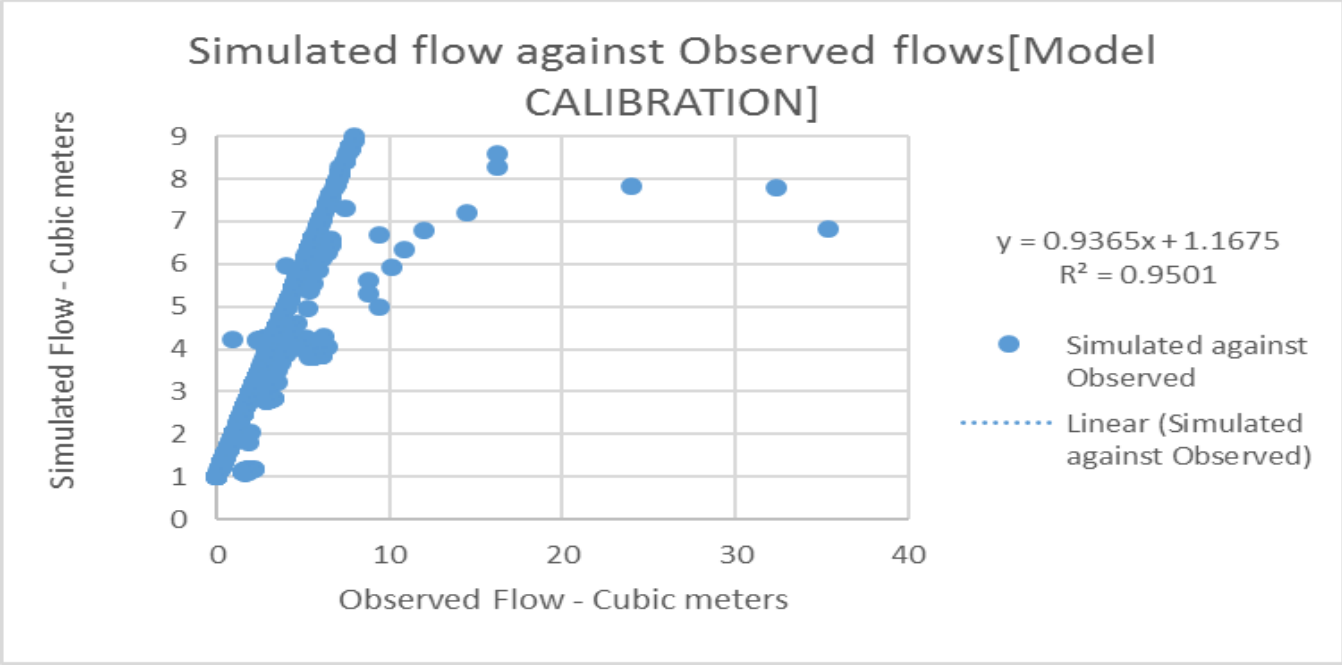

Figure 4.1: Simulated against Recorded Flows - Thika catchment

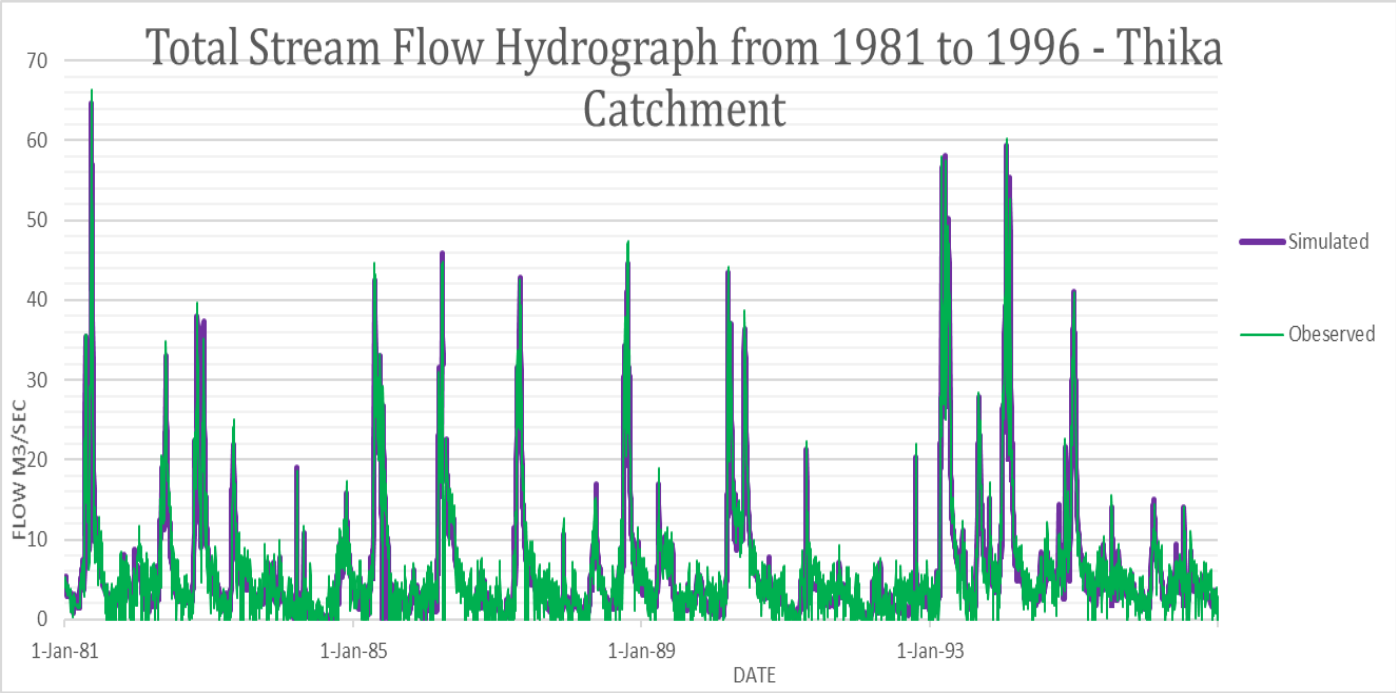

Figure 4.2 Total Stream Flow Hydrograph from 1981 to 1996 - Thika Catchment

According to Santhi et al., (2001), higher values of R^2 indicate less error variance and typically values greater than 0.50 are considered acceptable. The simulated and observed data for the year 1981 is presented in Table 4.4 and the subsequent period of calibration on Appendix 1.

Table 4.4: Recorded and Simulated flows from Calibration Process (Year 1981)

Series name	**Simulated**	**Recorded**
Series type	Flow	Flow
Units	Cumecs	Cumecs
Jan	0.448	3.554
Feb	0.41	2.301
Mar	4.859	3.05

Apr	31.948	16.405
May	23.556	28.668
Jun	10.185	9.024
Jul	6.25	4.366
Aug	3.421	2.752
Sep	1.845	2.179
Oct	1.18	2.557
Nov	8.974	3.904
Dec	7.46	4.295

4.3.2 HYSIM Validation for the period 1960 - 1964

The HYSIM model was validated using stream flow data from 1960 – 1964 and a coefficient of determination (R^2) obtained of value 0.916 as shown in Figure 4.3 and visually presented in figure 4.4. This value also corresponds to results obtained by Murphy and Charlton (2006) who obtained a value between 0.67 and 0.79

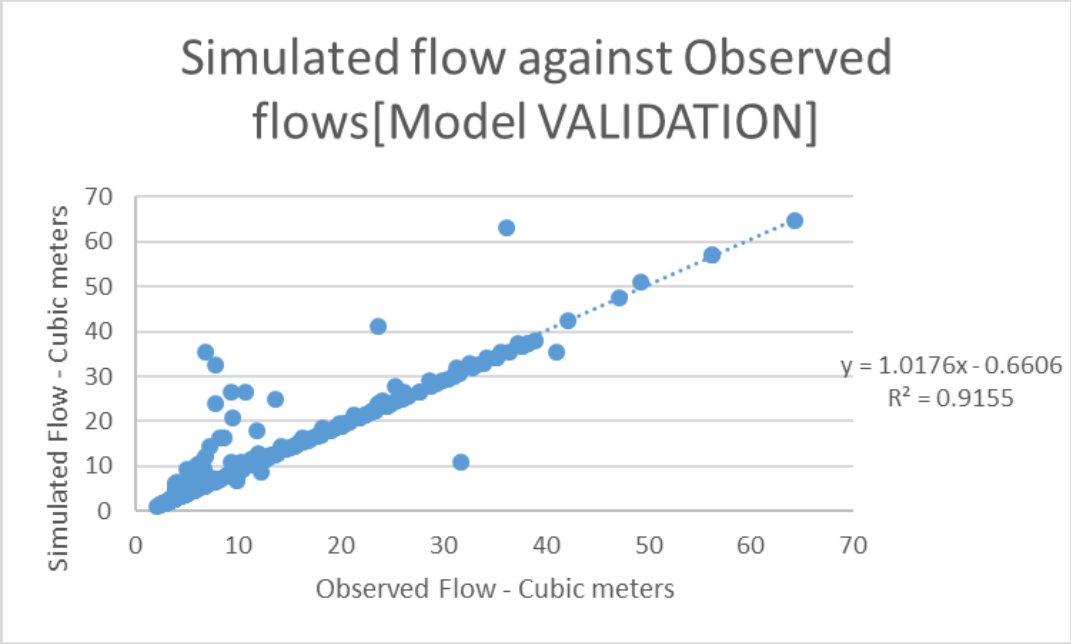

Figure 4.3: Simulated against Recorded Flows – Thika river catchment

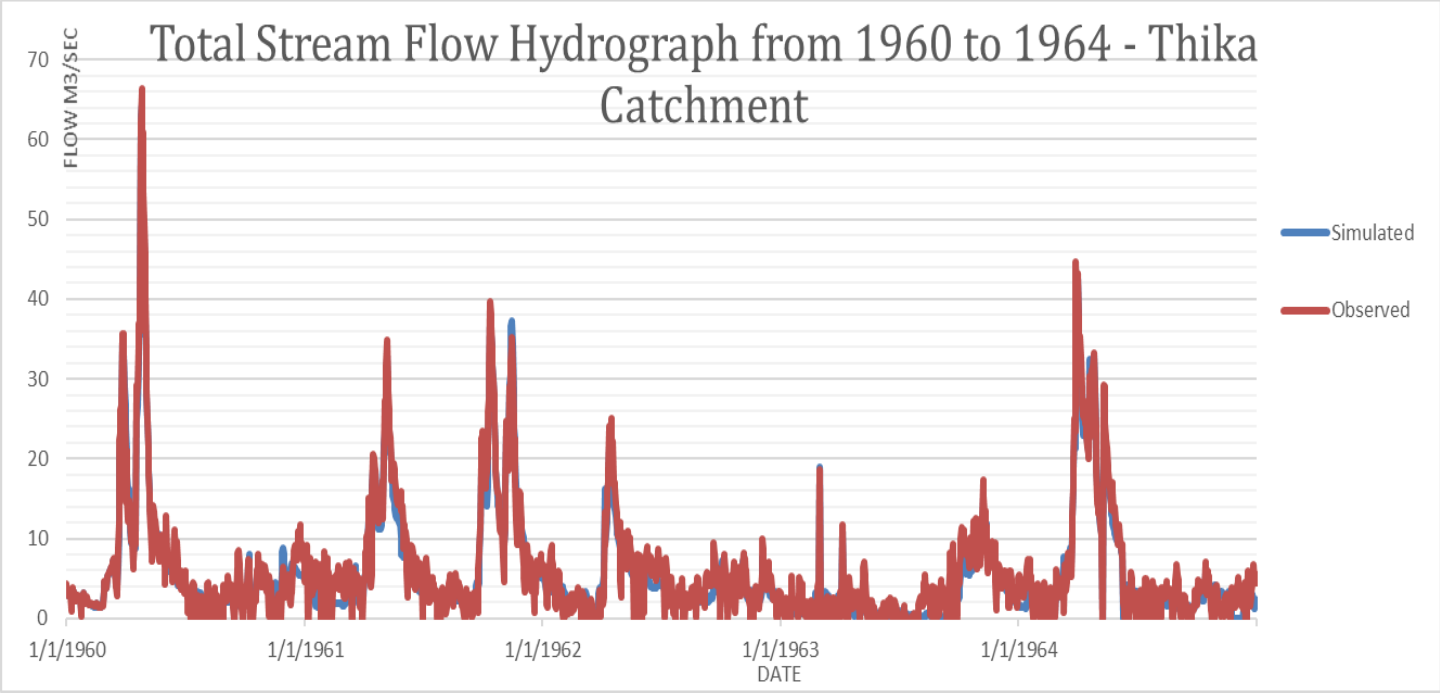

Figure 4.4 Total Stream Flow Hydrograph from 1960 to 1964 - Thika Catchment

The simulated and observed data for the year 1964 is presented in Table 4.5 the subsequent period of validation on Appendix 2.

Table 4.5: Recorded and Simulated flows from the Validation Process (Year 1964)

Series names	**Simulated**	**Recorded**	**Bias**	**MAE**
Series types	Flow	Flow		
Units	Cumecs	Cumecs		
Jan	4.63	4.54	0.10	0.0956
Feb	4.18	4.65	-0.48	0.476
Mar	4.18	4.02	0.16	0.157
Apr	5.10	4.98	0.12	0.118

May	5.34	5.33	0.02	0.0166
Jun	4.40	4.33	0.08	0.078
Jul	4.25	4.25	-0.01	0.0068
Aug	4.09	4.55	-0.45	0.453
Sep	3.94	3.87	0.07	0.073
Oct	3.78	3.75	0.03	0.0308
Nov	3.63	3.52	0.10	0.104
Dec	3.47	3.45	0.02	0.02
MAE & BIAS			-0.004	0.14

The results for the calibration and validation stages of the HYSIM model are detailed in Table 4.6.

Table 4.6 Calibration and validation results

Catchment Name	Measured Average Calibration	Simulated Average Calibration	Calibration (1981 - 1995)	Measured Average Validation	Simulated Average Validation	Validation (1960 - 1964)
			R^2			R^2
Thika Catchment	5.8	6.3	0.95	4.3	5.6	0.92

The results of the calibration and validation stage were very encouraging and showed that the HYSIM model was performing extremely well over the full period of record. The performance criteria is as summarized in Table 4.7.

Table 4.7: Performance criteria for calibration and validation.

Statistic	Calibration		Validation	
	Value	Performance	Value	Performance
BIAS	1.697	Good	-3.72	satisfactory
RMSE	0.56	Satisfactory	0.61	Not satisfactory
NSE	0.95	Very good	0.92	Very good

4.4 Surface Runoff – Comparative period

The surface runoff for the comparative period of 2017-2021 was simulated and is presented below graphically in Figure 4.3 and tabulated in Table 4.6.

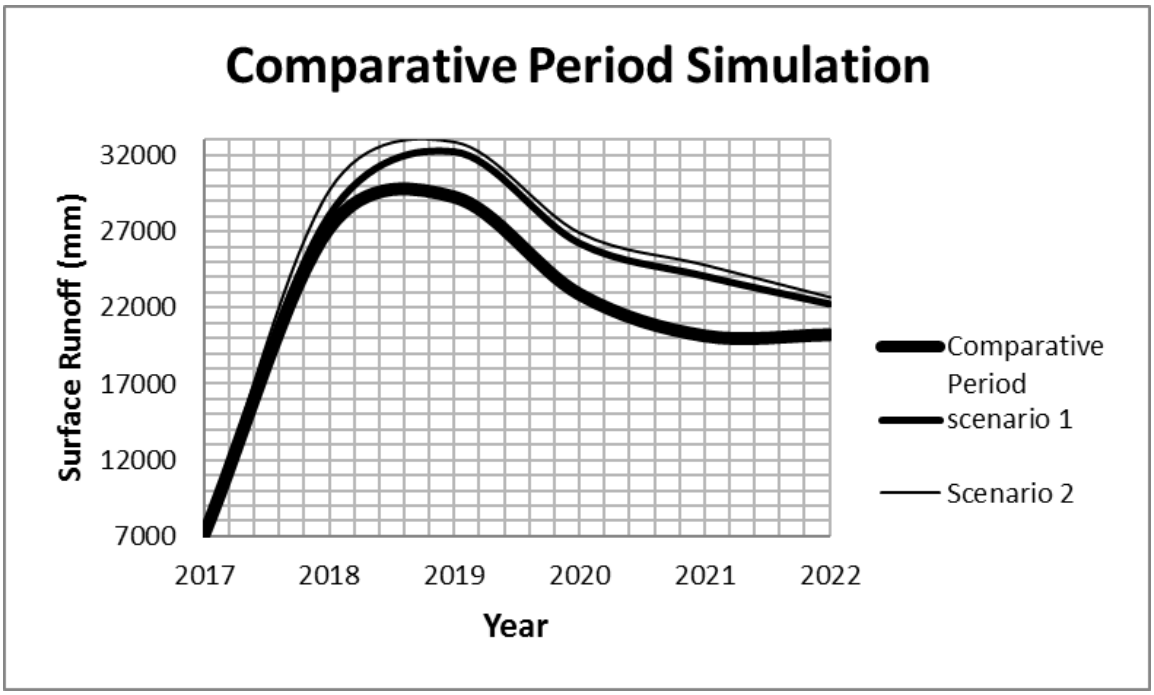

Figure 4. 2: Comparative period graphical representation

Table 4.6: Surface Runoff - Comparative (Year 2017 - 2022)

Year	Comparative Period (mm)	Scenario 1 (mm)	Change between Sc.1 and the Comparative period	Scenario 2 (mm)	Change between Sc.1 and the Comparative period
2017	7135	7185	50	7310	175
2018	27448	28026	578	29753	2305
2019	32041	32257	216	32902	861
2020	25995	26242	247	26932	937
2021	23823	24074	251	24830	1007
2022	22062	22241	179	22719	657
	Total		1524		5943

The two scenarios described in the methodology were carried out and the comparative period runoff simulated. Further analysis of the runoff simulated indicated that in both scenarios (both

high and low) there was an increase. In the low scenario an increase of 1524 mm over the comparative period was observed. This was an increase of 1.2% in surface runoff over the comparative period. In the high scenario an increase of 5943 mm over the comparative period was observed. This was an increase of 4.5% in surface runoff over the comparative period. Since the climate variability changes and trends in the catchment are potentially a result of global climate change, the future climate, including rainfall and temperature, is of utmost interest to water resource management and planning, agriculture, and water users in the region. The scenarios used in this study were results of climate change studies by IPCC in the region. This change in the main climate change drivers (temperature and precipitation) were developed using the Second Generation Global Climate Model. In both cases the GCM's prediction was that both temperature and precipitation would increase. This confirms results I obtained from the trend analysis that indicated increase over the past three decades. Thus an increase in precipitation in the catchment coupled by an increase in temperatures can still result in a projected increase of stream flow. This will produce a serious challenge for water resources management in the NCP region and enhance the vulnerability of water resources.

4.5 Trend analysis

4.5.1 Rainfall trends and magnitude

Both Mann Kendell and Sen's slope estimate tests were carried on the 30-year rainfall data for the period between 1976 and 2006. The results illustrate that rainfall desiccation of the early 1980s established by Hulme (2000) and Nicholson et al (1999) in Sahelian region also affected the Great Horn of Africa. The results are presented in t Table 4.7.

Table 4.7: Mann Kendell and Sen's slope estimate tests results

Time series	First year	Last Year	n	Test Z	Significance	Q	Mean Monthly Rainfall	Min Monthly Rainfall - mm	Max Monthly Rainfall - mm
Jan	1976	2006	31	0.07		0.063	56.9	0.0	358.4
Feb	1976	2006	31	-0.17		-0.050	44.7	0.0	236.1
Mar	1976	2006	31	-0.82		-1.238	118.0	6.3	318.5
Apr	1976	2006	31	0.44		1.500	216.4	5.0	487.2
May	1976	2006	31	1.67	+	2.960	107.7	0.6	357.5
Jun	1976	2006	31	-1.67	+	-0.311	34.6	0.9	343.3
Jul	1976	2006	31	-1.17		-0.208	16.0	0.0	94.3
Aug	1976	2006	31	0.00		0.000	17.7	0.0	212.3
Sep	1976	2006	31	-1.05		-0.192	18.6	0.0	80.2
Oct	1976	2006	31	-0.03		-0.150	92.1	2.8	248.9
Nov	1976	2006	31	1.29		3.041	174.9	2.1	422.6
Dec	1976	2006	31	0.41		0.678	100.0	12.1	243.1
Annual	1976	2006	31	0.78		0.348	56.9	0.0	358.4

Overall, the Kendall's test results show a slightly increasing trend for annual precipitation, although it is not statistically significant as displayed on Figure 4.4.

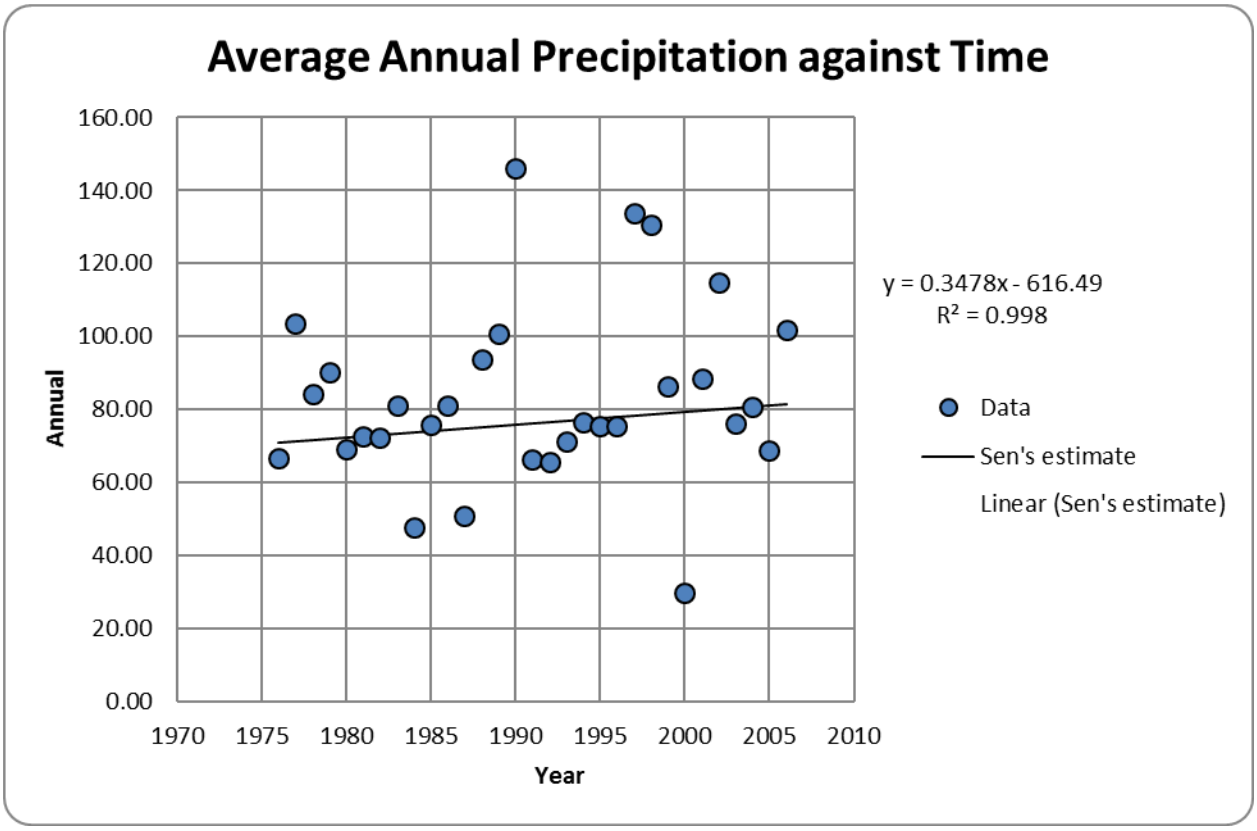

Figure.3.4: Average annual precipitation against time

This is in agreement with the findings by Yue *et al*. (2002). The magnitude of the precipitation trend from Sen's slope indicates that overall the annual precipitation in the catchment has increased by 7.8mm in the last 30 yrs. A summary of the trend analysis results is as present on Table 4.8.

Table 4.8: Summary of statistical analysis on Rainfall trend

Years	**1976 - 2006**
No of years	31
Test Z	0.78
Significant	Not

4.5.2 Temperature trends and magnitude

Both Mann Kendell and Sen's slope estimate tests were carried on the 30-year temperature data as presented in table 4.8.

Table 4.8: Mann Kendell and Sen's slope estimate tests results

Time series	First year	Last Year	n	Test Z	Significance	Q	Mean Monthly Temp	Min Monthly Temp – ^{0}c	Max Monthly Temp – ^{0}c
January	1976	2006	30	0.35		0.004	19.7	18.0	20.8
February	1976	2006	30	0.09		0.000	20.4	17.6	21.5
March	1976	2006	30	0.93		0.020	21.2	19.8	22.5
April	1976	2006	30	1.44		0.028	20.9	19.8	22.1
May	1976	2006	30	1.15		0.017	20.2	18.3	22.1
June	1976	2006	30	0.31		0.005	18.8	17.8	20.6
July	1976	2006	30	0.02		0.000	17.8	16.8	19.3
August	1976	2006	30	1.19		0.021	18.1	17.0	19.3
September	1976	2006	30	1.39		0.019	19.5	18.2	20.5
October	1976	2006	30	1.22		0.023	20.5	19.6	21.7
November	1976	2006	30	0.60		0.010	20.1	19.3	23.4
December	1976	2006	30	1.96	*	0.031	19.7	18.8	20.9
Annual Mean	1976	2006	30	2.14	*	0.018			

The results of Kendall's test show that the climate of Thika Catchment has become warmer during the last three decades. From Figure 4.5 results show that the annual means of daily temperature have increased in the last three decades.

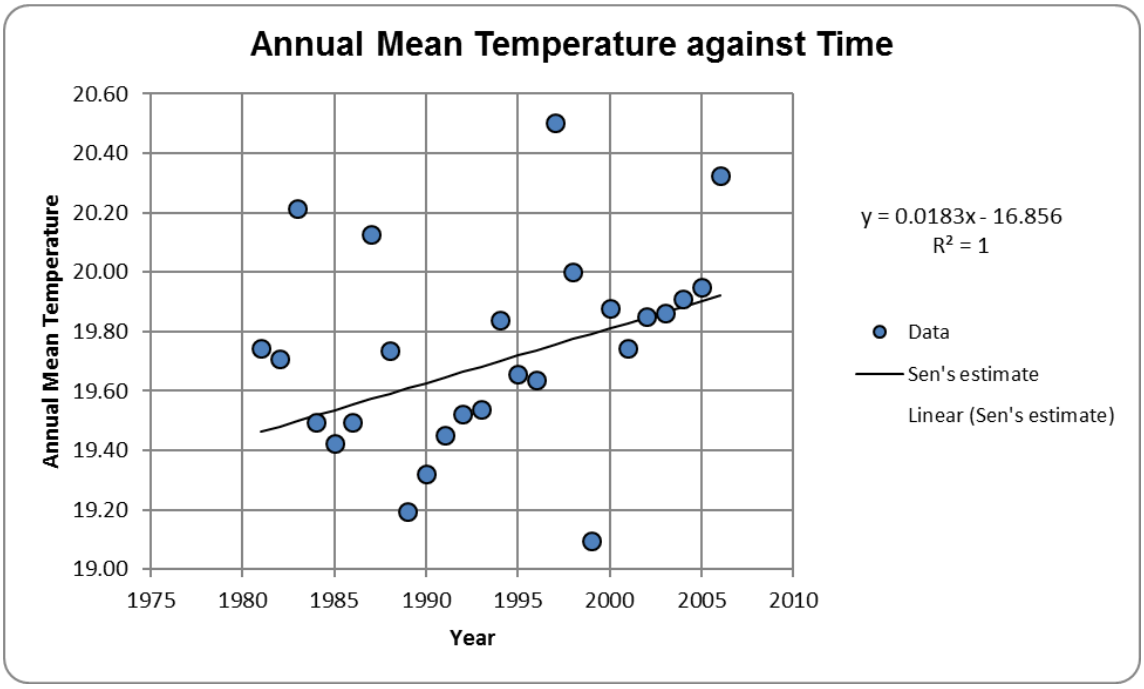

Figure 4.4: Annual mean temperatures against time

The Kendall analysis showed a statistically significant increasing trend during the last three decades (Fig. 4.5.) at α=0.05 level. A statistically significant trend in daily minimum temperature, or in the range of maximum and minimum daily temperature, is to be expected as an indicator of a global warming signal (Karl et al. 1993). The magnitude of the temperature trend from Sen's slope indicates that overall, the mean temperature in the catchment has increased by 2.14°c in the last 30 yrs. A summary of the results is a shown on Table 4.9.

Table 4.9: Summary of statistical analysis on Temperature trend

Years	**1976 - 2006**
No of years	30
Test Z	2.14
Significant	yes

CHAPTER FIVE

CONCLUSIONS AND RECOMMENDATIONS

5.1 Conclusions

i. Rainfall amounts and the mean annual temperatures were found to have increased in Thika catchment in the last four decades by about 7.8 mm (although not statistically significant), and 2.14°C respectively. This was a clear indication that climatic variability has been occurring in the catchment and affecting levels of runoff produced into the rivers. There is reasonable evidence that some of the warming in the catchment is a result of global warming.

ii. The HYSIM model proved to be a near perfect model for simulating runoff within the catchment. Upon calibration the model gave a coefficient of determination of 0.923 which was confirmed upon validation with a value of 0.916.

iii. The scenario analysis on the comparative period showed that surface runoff will increase with between 1524 mm and 5943 in the coming 5 years. Intensive water resource management is therefore required to ensure minimal loss as well as conservation of this precious resource.

5.2 Recommendations

i. The stream flow data quality and its consistency available at WRMA very poor. This can be partly blamed on the vandalism of river flow gauges in the catchment. Automatic/real-time river flow stations should be employed to capture weather data for the catchment.

ii. Nairobi water company should build more water harnessing dams or alternatively expand the existing Ndakaini dam in the catchment. This will ensure that the excess runoff is captured and hence more water to the city residents.

iii. More research on land use changes needs to be done. Thika town has become more urbanized which is factor to consider in studying increased flow within catchment.

Bibliography

Abbaspour, K. C., Yang, J., Maximov, I., Siber, R., Bogner, K., Mieleitner, J., ... & Srinivasan, R. (2007). *Modelling hydrology and water quality in the pre-alpine/alpine Thur watershed using SWAT*. *Journal of hydrology*, *333*(2), 413-430.

Ahmad, S., & Simonovic, S. P. (2000). System dynamics modeling of reservoir operations for flood management. *Journal of Computing in Civil Engineering*, *14*(3), 190-198.

Barnett, T.P, Pierce, D.W., Hidalgo, H.G., Bonfils C., Santer, B.D., Das, T., Bala, G., Wood, W.A., Nozawa, T., Mirin, A.A., Cayan, D.R., and Dettinger, M.D. (2008). Human Induced Changes in the Hydrology of the Western United States. *Science*, 139, 1080-108.

Beven, K. (1989). Changing ideas in hydrology—the case of physically-based models. *Journal of hydrology*, *105*(1), 157-172.

Box GE, Jenkins GM (1970). *Time series analysis: forecasting and control*, Holden-Day, Inc., San Francisco, CA.

Casella, G., and Berger, R.L. (1990). *Statistical Inference*. Pacific Grove, California: Wadsworth and Brooks/Cole.

Christensen, J.H., Hewitson, B., Busuioc, A., Chen, A., Gao, X., Held, I., Jones, R., Kolli, R.K., Kwon, W.-T., Laprise, R., Magaña Rueda, V., Mearns, L., Menéndez, C.G., Räisänen, J., Rinke, A., Sarr, A. and Whetton, P. 2007. Regional Climate Projections. In: Solomon, S., Qin, D., Manning, M., Chen, Z., Marquis, M., Averyt, K.B., Tignor, M. and Miller, H.L. (eds.) Climate Change 2007: The Physical Science Basis. Contribution of Working Group I to the Fourth Assessment Report of the Intergovernmental Panel on Climate Change. Cambridge University Press, Cambridge, UK.

Climate Data Information (2015), *Climate Data Information Examples of HYSIM-CC Model Use: Turkey,* Climatedata.info, Retrieved 29th Dec., 2015, from, http://www.climatedata.info/HYSIMCC/examples/

Dooge J.C.I., (1973). *Linear Theory of hydrologic systems*. Tech. Bull. 1468. Agric. Res. Service, US Dept. Agric., Washington.

Droogers, P., & Kite, G. (1999). Water productivity from integrated basin modeling. *Irrigation and Drainage Systems*, *13*(3), 275-290.

Frederick, K. D., & Gleick, P. H. (1999). *Water & global climate change: potential impacts on US water resources*. Pew Center on Global Climate Change.

Fu, G., Charles, S. P., Yu, J., & Liu, C. (2009). Decadal climatic variability, trends, and future scenarios for the North China Plain. *Journal of Climate*, *22*(8), 2111-2123.

Gathenya, J. (1999). *Einsatz Von Waseerhausmodellenzurwasserbewirt-schaftung am Beispiel des Thika- Chania-Gebietes in Kenya.* Institute of Hydraulic Eng and Water Mgt, University of Kaisserslauten. Kaisserslauten: Institute of Hydraulic Eng and Water Mgt, University of Kaisserslauten.

Hamed, K. H. (2008). Trend detection in hydrologic data: the Mann–Kendall trend test under the scaling hypothesis. *Journal of Hydrology*, *349*(3), 350-363.

Hay, S.I., Cox, J., Rogers, D.J., Randolph, S.E., Stern, D.I., Shanks, G.D., Myers, M.F. and Snow, R.W., (2002). Climate change and the resurgence of malaria in the East African highlands. *Nature*, *415*(6874), pp.905-909.

Hulme, M., Doherty, R.M., Ngara, T., New, M.G. and Lister, D. 2001. African climate change: 1900–2100. Climate Research 17(2): 145–168.

IPCC, Center, H. E., Engineers, U. A., & Davis. (2000). *Third and Second assessment reports.* California: IPCC.

IPCC. (n.d.). *Intergovernmental Panel on Climate Change (IPCC)*. Technical papers for Intergovernmental Panel on Climate Change (IPCC): Retrieved 29th Dec. 2015, from https://www.ipcc.ch/pdf/technical-papers/ccw/executive-summary.pdf

Jacobs, Sutton, R., Price, D. and McGregor, L., (2010). *Testing the sensitivity of surface water yields to the derivation of Hysim inflows*. Glasgow: Jacobs Engineering U.K. Ltd.

Jactzold, R. (1983). Natural conditions and farm mgt information. In R. Jactzold, *Part B-Central Kenya (R.Valley and Central Provinces)* (p. vol II). Nairobi: Ministry of Agriculture.

John Walker Recha, Bancy M. Mati, Mary Nyasimi, Philip K. Kimeli, James M. Kinyangi & Maren Radeny (2016) Changing rainfall patterns and farmers' adaptation through soil water management practices in semi-arid eastern Kenya, Arid Land Research and Management, 30:3, 229-238, DOI: 10.1080/15324982.2015.1091398

J.Wei, L.Chan, J.Chang, (2016). Runoff change in upper reach of Yellow River under future climate change based on VIC model. Journal of Engineering. DOI: 10.11660/slfdxb.20160508

Kenya Meteorological Department. (2010). *Climatological statistics for Kenya.* Nairobi: KMD.

KNMI. 2006. *Climate change in Africa. Changes in extreme weather under global warming, Royal Netherlands Institute of Meteorology*. http://www.knmi.nl/africa_scenarios/.

Lins, H., & Slack, J.R. (1999). Stream flow trends in the United States. *Geophysical Research Letters, 26*, 227-230.

Linsley, R. (1972). *Hydrology for Engineers* (3rd ed.). Singapore: McGraw- Hill International Book Company.

Luijten, J. (1999). *A tool for community based water resources in hillside watersheds.* Gainesville,FL: University of Florida.

Lukeman, A. (2003). *Regional impact of climate change and variability on water resources: case study of Lake Naivasha basin.* Kenya.

Lvovitch, M. (1972). *World water balance.* UNESCO.

Maidment, D. R. (1992). *Grid Based Computation of Runoff: A Preliminary Assessment*. Hydrologic Engieering Center.

Manley, R.E. (1993). *HYSIM Reference Manual*. R.E. Manley Consultancy, Cambridge. 63pp.

Manley, R.E., (2006). *A Guide to Using Hysim. Wallingford: Water Resource Associates Ltd.*

Michael D. & Cayan, R. (1995). The role of climate in estuarine variability. *American Scientist ;(United States), 83(1).*

Milan Gocic, Slavisa Trajkovic (2012). Analysis of changes in meteorological variables using Mann-Kendall and Sen's slope estimator statistical tests in Serbia. *Science direct*.

Millennium Ecosystem Assessment. 2005. *Ecosystems and Human Well-being*. Volume 1: Current State and Trends Assessment. Millennium Ecosystem Assessment. Island press.

Miller, K. A. (1997). *Climate Variability, Climate Change and Western Water*. Report to the Western Water Policy Review Advisory Commission, NTIS, Springfield, VA

Mogaka, H. (2006). *Climate variability and water resources degradation in Kenya: improving water resources development and management* (Vol. 69). World Bank Publications.

Moore, N., Alagarswamy, G., Pijanowski, B., Thornton, P.K., Lofgren, B., Olson, J., Andresen, J., Yanda,P., Qi, J. and Campbell, D. 2009. *Food production risks associated with land use change and climate change in East Africa. IOP Conference Series: Earth and Environmental Science 6*, 342003.doi:10.1088/ 1755-1307/6/4/342003.

Moradkhani, H. and Sorooshian, S., 2008. *General review of rainfall-runoff modeling: model - calibration, data assimilation, and uncertainty analysis. Hydrological modeling and the water cycle.* Springer. 291 p. ISBN 978-3-540-77842-4.

Murphy, C., & Charlton, R. (2006). *Climate Change Impact on Catchment Hydrology & Water Resources for Selected Catchments in Ireland*. Irish Climate Analysis and Research UnitS (ICARUS), NUI Maynooth. National hydrology conference.

Ndirangu, W. Kabubi, J. & Dulo, S. (2009). *Manual for hydro-climatic disasters in water resource management.* Nairobi: Water Resource Management Authority.

NEMA. (2014). *Climate change impacts/vulnerability assessments and adaptation options.* Nairobi: National Environment Management Authority.

NERC, (1975). *Flood Studies Report*. Institute of Hydrology, NERC. UK.

Osbahr, H. and Viner, D. 2006. *Linking Climate Change Adaptation and Disaster Risk Management for Sustainable Poverty Reduction. Kenya Country Study. A study carried out for the Vulnerability and Adaptation Resource Group (VARG) with support from the European Commission.*

Pacini N., & Harper D.M. (1998). *The Sustainable Management of Tropical Catchments.*

Parry, M. L. (Ed.). (2007). *Climate change 2007-impacts, adaptation and vulnerability: Working group II contribution to the fourth assessment report of the IPCC* (Vol. 4). Cambridge University Press.

Philip J.R., (1957). The theory of infiltration, 1 The infiltration equation and its solution. *Soil Sci.*, 83(1), 345-357.

Ray, K., (1975). *Hydrology for Engineers*. McGraw Hill Kogakusha.

Refsgaard, C. (1996). Parameterization, calibration and validation of distributed hydrological models. *Journal of hydrology*(198), 69-67.

Santhi, C., Arnold J. G., Williams, J. R., Dugas, W. A., Srinivasan, R. and Hauck, L. M. (2001). Validation of the SWAT model on a large river basin with point and nonpoint sources. *Journal of American Water Resources Association*, 37: 1169-1188.

Scottish Water, 2009. Scottish Water Resource Plan. Dunfermline: Scottish Water.

Seager, R., Ting, M., Held, I., Kushnir, Y., Lu, J., Vecchi, G., ... & Li, C. (2007). Model projections of an imminent transition to a more arid climate in southwestern North America. *science*, *316*(5828), 1181-1184.

Sen, P. K. 1968. *Estimates of the regression coefficient based on Kendall's Tau. Journal of the American Statistical Association*, 63(324), 1379-1389. [doi:10.1080/01621459.1968.10480934]

Singh, V. P. (1995). *Computer models of watershed hydrology*. Water Resources Publications.

Stocker, T.F., Qin, D., Plattner, G.K., Tignor, M., Allen, S.K., Boschung, J., Nauels, A., Xia, Y., Bex, V. and Midgley, P.M., 2014. *Climate change 2013: The physical science basis*.EPA lecture series.

Su, F., Hong, Y., & Lettenmaier, D. P. (2008). *Evaluation of TRMM Multisatellite Precipitation Analysis (TMPA) and its utility in hydrologic prediction in the La Plata Basin.* *Journal of Hydrometeorology, 9(4), 622-640.*

US Army Corps of Engineers, (2011). *What's New? Version 3.0 (April 2007) of the Reservoir System Simulation program (HEC-ResSim).* Retrieved 10th February 2016 from, http://www.hec.usace.army.mil/software/hec-ressim/whats_new.html

Wambua RM, Mutua BM, Raude JM (2014). Drought Forecasting Using Indices and Artificial Neural Networks for Upper Tana River Basin, Kenya-A Review Concept. *J Civil Environ Eng 4: 152. doi:10.4172/2165-784X.1000152*

Westmacott, J.R., & Burn, D.H. (1997). Climate change effects on the hydrologic regime within the Churchill-Nelson River Basin. *Journal of Hydrology*(202), 263-279.

Appendix

Appendix 1 – Simulated and Observed monthly mean values for the calibration period – 1982 - 1995

Year	Simulated Flows	Observed Flows
Jan-82	3.53	8.40
Feb-82	3.74	9.07
Mar-82	3.32	7.40
Apr-82	3.32	6.77
May-82	3.32	5.03
Jun-82	3.32	3.59
Jul-82	3.11	2.64
Aug-82	3.11	1.60
Sep-82	2.91	1.29
Oct-82	3.53	4.97
Nov-82	3.53	3.69
Dec-82	3.32	4.32
Jan-83	4.40	5.87
Feb-83	4.18	5.60
Mar-83	3.53	3.78
Apr-83	3.32	3.72
May-83	3.11	3.49
Jun-83	3.53	2.85
Jul-83	3.96	2.19

Aug-83	3.74	0.41
Sep-83	3.32	-0.32
Oct-83	3.11	1.65
Nov-83	2.91	2.09
Dec-83	2.72	0.46
Jan-84	2.72	2.17
Feb-84	2.72	2.43
Mar-84	2.53	2.59
Apr-84	1.03	0.64
May-84	1.81	2.32
Jun-84	1.81	1.98
Jul-84	1.81	1.98
Aug-84	1.81	2.97
Sep-84	1.81	0.76
Oct-84	1.81	3.01
Nov-84	1.81	2.31
Dec-84	1.81	1.04
Jan-85	1.81	1.61
Feb-85	1.81	2.97
Mar-85	1.81	3.08
Apr-85	1.81	2.84
May-85	1.81	2.55
Jun-85	1.81	3.86

Jul-85	1.81	3.07
Aug-85	1.81	1.70
Sep-85	1.81	1.66
Oct-85	1.64	2.36
Nov-85	1.64	1.91
Dec-85	1.64	-0.56
Jan-86	1.64	3.29
Feb-86	1.81	2.92
Mar-86	1.81	2.99
Apr-86	1.81	2.34
May-86	2.34	2.16
Jun-86	3.11	0.90
Jul-86	3.32	1.44
Aug-86	2.91	-0.89
Sep-86	2.16	-2.44
Oct-86	1.98	-1.78
Nov-86	1.64	-2.27
Dec-86	1.33	-2.00
Jan-87	1.33	0.39
Feb-87	1.18	0.81
Mar-87	1.64	2.36
Apr-87	1.64	1.76
May-87	1.33	1.03

Jun-87	1.03	0.06
Jul-87	1.03	-0.82
Aug-87	1.03	-0.82
Sep-87	1.03	-2.38
Oct-87	1.03	-0.86
Nov-87	1.03	-1.43
Dec-87	1.33	-1.49
Jan-88	1.18	-0.85
Feb-88	1.33	-1.44
Mar-88	3.11	0.76
Apr-88	3.74	3.49
May-88	1.18	0.33
Jun-88	1.33	1.39
Jul-88	3.11	2.47
Aug-88	3.74	1.73
Sep-88	4.40	1.65
Oct-88	5.34	2.68
Nov-88	7.39	4.99
Dec-88	16.19	13.25
Jan-89	9.42	9.09
Feb-89	10.50	11.69
Mar-89	12.16	13.82
Apr-89	13.82	16.01

May-89	15.48	17.15
Jun-89	17.13	18.98
Jul-89	21.89	24.12
Aug-89	18.01	19.23
Sep-89	15.75	17.78
Oct-89	20.89	25.06
Nov-89	19.43	22.38
Dec-89	17.09	22.19
Jan-90	15.32	17.33
Feb-90	14.04	16.89
Mar-90	13.63	16.95
Apr-90	13.63	16.30
May-90	12.81	14.32
Jun-90	11.25	13.13
Jul-90	10.50	12.13
Aug-90	10.50	10.29
Sep-90	10.14	10.78
Oct-90	9.42	10.43
Nov-90	8.73	12.09
Dec-90	8.39	4.62
Jan-91	7.74	2.67
Feb-91	7.74	7.11
Mar-91	7.39	10.78

Apr-91	7.74	10.17
May-91	7.74	9.61
Jun-91	6.86	8.44
Jul-91	6.60	6.41
Aug-91	6.34	7.40
Sep-91	6.34	6.18
Oct-91	6.43	7.50
Nov-91	6.51	8.72
Dec-91	6.60	10.93
Jan-92	6.60	8.70
Feb-92	6.39	10.02
Mar-92	6.17	9.29
Apr-92	5.96	8.15
May-92	5.71	7.77
Jun-92	5.46	8.00
Jul-92	5.34	6.89
Aug-92	5.34	5.43
Sep-92	5.11	-3.25
Oct-92	4.87	3.83
Nov-92	4.63	5.50
Dec-92	4.40	5.31
Jan-93	4.40	6.53
Feb-93	4.52	7.96

Mar-93	4.18	-0.57
Apr-93	4.18	6.03
May-93	4.18	7.30
Jun-93	4.18	7.86
Jul-93	4.18	4.46
Aug-93	4.18	6.64
Sep-93	4.87	-0.73
Oct-93	5.34	7.11
Nov-93	5.83	2.97
Dec-93	6.09	0.78
Jan-94	5.34	3.89
Feb-94	5.59	7.08
Mar-94	5.83	7.42
Apr-94	6.34	7.95
May-94	6.34	9.00
Jun-94	5.59	7.90
Jul-94	5.10	7.94
Aug-94	4.63	6.40
Sep-94	4.40	6.04
Oct-94	4.18	6.49
Nov-94	3.96	7.71
Dec-94	3.96	5.37
Jan-95	3.74	7.22

Feb-95	3.74	7.03
Mar-95	3.74	6.58
Apr-95	3.74	6.26
May-95	3.96	5.70
Jun-95	3.74	5.58
Jul-95	3.96	4.74
Aug-95	4.63	6.12
Sep-95	5.10	5.68
Oct-95	4.63	8.66
Nov-95	4.40	6.92
Dec-95	4.18	5.83

Appendix 2 – Simulated and Observed monthly mean values for the validation period – 1960 - 1963

Year	Simulated	Observed
Jan-60	0.88	1.26
Feb-60	0.88	1.53
Mar-60	0.80	1.59
Apr-60	0.80	4.40
May-60	0.74	5.81
Jun-60	0.74	6.27
Jul-60	0.74	5.02
Aug-60	0.74	4.39

Sep-60	0.74	2.65
Oct-60	0.74	1.21
Nov-60	0.88	0.60
Dec-60	0.80	0.51
Jan-61	0.74	0.69
Feb-61	0.88	2.52
Mar-61	0.74	1.10
Apr-61	0.80	2.01
May-61	0.88	2.55
Jun-61	0.95	2.57
Jul-61	0.95	1.40
Aug-61	0.88	1.48
Sep-61	0.80	1.38
Oct-61	0.88	0.41
Nov-61	0.74	0.83
Dec-61	0.74	2.39
Jan-62	0.74	2.70
Feb-62	0.74	0.53
Mar-62	0.95	0.33
Apr-62	1.36	0.70
May-62	1.63	1.29
Jun-62	2.45	2.37
Jul-62	2.23	2.49

Aug-62	2.02	1.83
Sep-62	1.92	2.63
Oct-62	1.72	2.10
Nov-62	1.72	2.10
Dec-62	1.63	2.99
Jan-63	1.45	0.60
Feb-63	1.54	2.94
Mar-63	1.45	2.15
Apr-63	1.36	0.79
May-63	1.36	1.36
Jun-63	1.45	2.81
Jul-63	1.36	2.84
Aug-63	1.27	2.50
Sep-63	1.72	2.66
Oct-63	1.72	3.97
Nov-63	1.63	3.09
Dec-63	1.45	1.54